Crowd motion from the granular standpoint

Sylvain Faure, Bertrand Maury

CROWD MOTION FROM THE GRANULAR STANDPOINT

SYLVAIN FAURE [#] AND BERTRAND MAURY [#]

[#] *Laboratoire de Mathématiques d'Orsay, Université Paris-Sud, France*

Abstract. Following the approach initially proposed in Maury & Venel [30, 31], we consider here crowd motion from the standpoint of granular media, and we investigate how theoretical and numerical tools in non-smooth analysis can help better understanding some paradoxical features. We shall be especially interested in evacuation processes, jams, and we will detail how the granular nature of the flow helps to understand two well-known phenomena, the so-called "Faster is Slower" effect, and "Stop-and-Go" waves.

1. Introduction

Most crowd motion models are based on the following fundamental ingredients:

(1) Individual projects: Pedestrians tend to achieve a certain objective, typically reach a certain zone (e.g. an exit door in case of emergency evacuation);
(2) Social tendencies: Each individual adapts its behavior according to the perception he has from its environment, in particular the location of other people. The best example is the tendency to keep at a certain distance away from neighbors. This "comfort" distance depends on many parameters, among which is the cultural background [16];
(3) Physical interaction: In overcrowded situations, actual contacts (between individuals, or with obstacles) may occur, and the resulting forces are likely to greatly affect the overall behavior of the crowd. This item is sometimes disregarded, but it will play a crucial role in the present paper.

Modeling strategies can be classified according to the manner they transform these principles into equations.

Macroscopic *vs.* microscopic. Both *microscopic* and *macroscopic* approaches can be carried out, depending on whether people are followed individually, or handled as a global entity. The *macroscopic* approach consists in conceiving the crowd as a whole, with no account of particular individuals. The associated mathematical object is a density function, that represents the local density of pedestrian. This density is transported by the global velocity field $\mathbf{u}$:

$$\frac{\partial \rho}{\partial t} + \nabla \cdot (\rho \mathbf{u}) = 0.$$

Designing a model amounts to set rules to define $\mathbf{u}$ at each instant. It can be defined in a traffic flow spirit [23] by setting $\mathbf{u} = \alpha \mathbf{U}$, where $\mathbf{U}$ is the desired velocity field ($\mathbf{U}(\mathbf{x})$ is the velocity that a single person at $\mathbf{x}$ would take), and $\alpha = \alpha(\rho)$ is a correction factor, that accounts for congestion: The velocity is reduced when the local density is high. Another

Keywords : crowd motion; microscopic modeling; congestion; stability of jams
AMS Subject Classification: 70E50, 70E55, 34D20, 92D50

MICRO	Soft	Hard
1^{st} order	Burstedde *et al.* [8] Schadschneider & Seyfried [41] Maury [27]	Maury & Venel [30, 31] Pécol, Dal Pont, Erlicher & Argoul [38]
2^{nd} order	Helbing [18, 17, 19, 20] Parisi, Gilman & Moldovan [37] Parisi & Dorso [36] Xi, Son & S. Lee [46] P. Degond, C. Appert-Rolland, J. Pettre & G. Theraulaz [12]	Granular flows [1, 35, 26] *(not implemented for crowd motions)*

TABLE 1. Microscopic models

choice consists in adding a PDE for the velocity: Euler-like equation with a forcing term that accounts for relaxation toward the desired velocity [2], or Darcy-like equation to account for congestion [28, 29].

In the *microscopic* setting, pedestrians are described individually, and direct (social or mechanical) interactions between any two neighboring individuals can be accounted for. The core of the model lies in the definition of individual velocities, in a way that integrates personal projects, social tendencies, and/or actual contacts with neighbors. This approach makes it possible to differentiate individuals, in terms of speed, strategy, etc .... Although they are not of the differential type, *Cellular Automata* methods [41, 8] fit in this class of microscopic models, since they allow to handle individual strategies.

Let us also mention an intermediate approach, based on a kinetic description of the crowds, which makes it possible to establish links between the different scales of description [3], and an alternative description based on time-evolving measures [39].

First order *vs.* second order. A second alternative lies in the dynamics: first order or second order in time ? As we shall detail further, the first microscopic models introduced by Helbing [17] were designed within the framework of classical mechanics: Individuals were identified to inertial objects. This leads to a second order in time equation on the position vector. Yet, a first order in time makes sense if one considers that individuals are able to move from rest and quasi-instantaneously achieve their desired velocity. It also allows nonsmooth trajectories (sudden change of direction), which are ruled out by second-order models. Besides, it reduces the number of parameters of the model, and suppresses unrealistic oscillations that are likely to be produced by inertial crowd models.
Soft *vs.* hard. A third alternative concerns the way direct interactions are handled. By direct interactions we mean actual contacts between individuals. They are likely to happen in highly crowded situations, especially during emergency evacuations involving panic. Like in the granular community, two options are possible: the *soft sphere* approach, also called Molecular Dynamics approach (MD) in physics, consists in applying short range forces between individuals, whereas in the Contact Dynamics approach, contacts are treated as non-smooth events (*hard* handling of congestion).

Tables 1 and 2 propose a classification of models in the literature, according to these three criteria. Except for Cellular Automata, we restricted the scope of this classification to differential models, i.e. models that take the form of Ordinary Differential Equations

MACRO	Soft	Hard
1^{st} order	Bellomo, Bellouquid & Knopoff [3] Hughes [23] Garavello & Lécureux-Mercier [10] Chalons, Goatin & Seguin [9] Burger, Markowich & Pietschmann [7] Piccoli & A. Tosin [39]	Maury, Roudneff-Chupin & Santambrogio [28]
2^{nd} order	Bellomo & Dogbé [2] Hoogendoorn & Bovy [21, 22]	Pressureless Euler eqs. with maximal density constraint [4, 6] *(not implemented for crowd motions)*

TABLE 2. Macroscopic models

(microscopic) or Partial Differential Equations (macro). We refer to the recent overview of alternative approaches proposed in Ref. [13]. Let us make a few remarks on this overview, in order to stress the deep differences between crowd motion and car traffic modeling.

(1) While first-order macroscopic models have been implemented in many ways, a large majority of microscopic model are of second order in time. The only first-order micro models in the literature are not of the differential type (Cellular Automata). The differential first order model described in Ref [27] is simply proposed as an alternative to second order models, but not really investigated.
(2) Actual contacts between individuals are commonly handled by a soft sphere approach (a short range force is added to penalize overlapping) whereas, in the granular community, a fair balance holds between Molecular Dynamics (soft) and Contact Dynamics (hard) strategies.
(3) Microscopic hard congestion second order model corresponds to standard granular flows. At the macroscopic level, hard congestion - second order models would correspond to the so-called Pressureless Euler equations with congestion constraint [4, 6]. None of these approaches have been implemented in the context of crowd motions.

The present paper is focused on the microscopic – 1rst order – hard approach that was initially proposed in Refs. [30, 31]. We shall present how this approach can be built as an asymptotic limit of Helbing's model [17], by having the relaxation time go to 0, and the stiffness go to $+\infty$. The limit models reflect the link between crowd motion and granular flows, which makes it particularly suitable to investigate highly packed crowds and jamming phenomena. This approach can be coupled with sophisticated strategies to model interaction between individual [44], including social tendencies (stay at a minimal distance from neighbors) or optimization (adaptation of one individual's desired velocity to develop personal optimization strategies, accounting for the behaviour of others). Yet, we have taken the choice to focus here on a purely *greedy* version of the model, disregarding any social tendency or sophisticated strategy. This model will simply include individual tendencies to reduce one's personal dissatisfaction, regardless of others, and the interaction between individual will be purely physical (i.e. actual contacts between the disks that represent people), due to the incompatibility of individual projects. We aim at showing in this manner that some observed effects, like *Stop-and-Go* waves or *Faster is Slower* effect, can be explained and even quantified from a purely granular standpoint, with very few parameters (in particular there will be no friction between individuals).

2. A hierarchy of microscopic models

We aim here at establishing links between the different types of microscopic models, starting from the seminal one proposed by Helbing in the early 90' (see Ref. [17]). We denote by

$$\mathbf{q} = (\mathbf{q}_1, \mathbf{q}_2, \dots, \mathbf{q}_N) \in \mathbb{R}^{2N}$$

the position vector, and by r_1, r_2, $\dots r_N$ the radii of individuals, considered as disks, and we define $\mathbf{U} \in \mathbb{R}^{2N}$ as the vector of desired (or spontaneous) velocities, i.e.

$$\mathbf{U} = (\mathbf{U}_1, \mathbf{U}_2, \dots, \mathbf{U}_N) \in \mathbb{R}^{2N},$$

where $\mathbf{U}_i$ is the desired velocity of individual i, in the selfish sense: it is the velocity that individual i would like to have if he were alone. The behavior of i is likely to be influenced by other people: this influence is accounted for by a correction term that is added to the right-hand side of the equation:

$$\ddot{\mathbf{q}} = \frac{1}{\tau}\left(\mathbf{U} - \dot{\mathbf{q}}\right) + \frac{1}{\tau}\mathbf{f}(\mathbf{q}).$$

The first term in the right-hand side reflects the tendency of individual to achieve their desired velocity (with a relaxation time $\tau > 0$), and the second one corresponds to interactions. Considering that this equation expresses Newton's Law for a system of particles, this term can be interpreted as a force (it is actually expressed in $\mathrm{N\,kg^{-1}}$), and the notion of *social forces* was indeed introduced in Ref. [17] to designate pairwise interations between individuals. We denote by $\mathbf{e}_{ij} = (\mathbf{q}_j - \mathbf{q}_i) \,/\, |\mathbf{q}_j - \mathbf{q}_i|$ the unit vector from i to j, a natural choice is

$$\mathbf{f}_i = -\kappa \sum_{j \neq i} \varphi(D_{ij})\, \mathbf{e}_{ij}\,, \text{ with } D_{ij} = |\mathbf{q}_j - \mathbf{q}_i| - r_i - r_j,$$

where $d \longmapsto \varphi(d)$ is a nonnegative, nonincreasing function, that expresses the tendency of people to stay apart from neighbors, and κ quantifies the effect of interactions. In order to alleviate notation, we do not explicitely integrate interactions with the environment (walls or obstacles), but they can be handled the same way (see Fig. 1). Let D^c_{ij} be the distance that individuals i and j consider as comfortable, and assume that $\kappa = U$ (magnitude of the typical desired velocity), φ can then be defined as

$$\varphi(d) = \exp\left(d/D^c_{ij}\right).$$

In this setting, interaction forces between i and j significantly affect the behaviour of i as soon as D_{ij} drops below the critical distance D^c_{ij}. Note that the interindividual distance that is considered as critical is likely to depend on the relationship between individuals, but also on cultural aspects. We refer to Hall [16] for a thorough account of the dependance of the critical distance (called *proxemy*) upon these factors.

In panic situations, interaction between individuals is likely to become less social: physical contacts happen. Accounting for these actual contacts calls for stiffer interaction terms. A penalty-like approach is proposed in Ref. [19], where a short range repulsive force is added to penalize overlapping between individuals (i.e. disks). The extra force is written

$$\mathbf{f}^c = \sum_{i \neq j} \kappa \left(r_i + r_j - |\mathbf{q}_j - \mathbf{q}_i|\right)_+ \mathbf{G}_{ij},$$

This notion of radius is somewhat sloppy unless individuals are identified to rigid disks, but it will help in quantifying interactions.

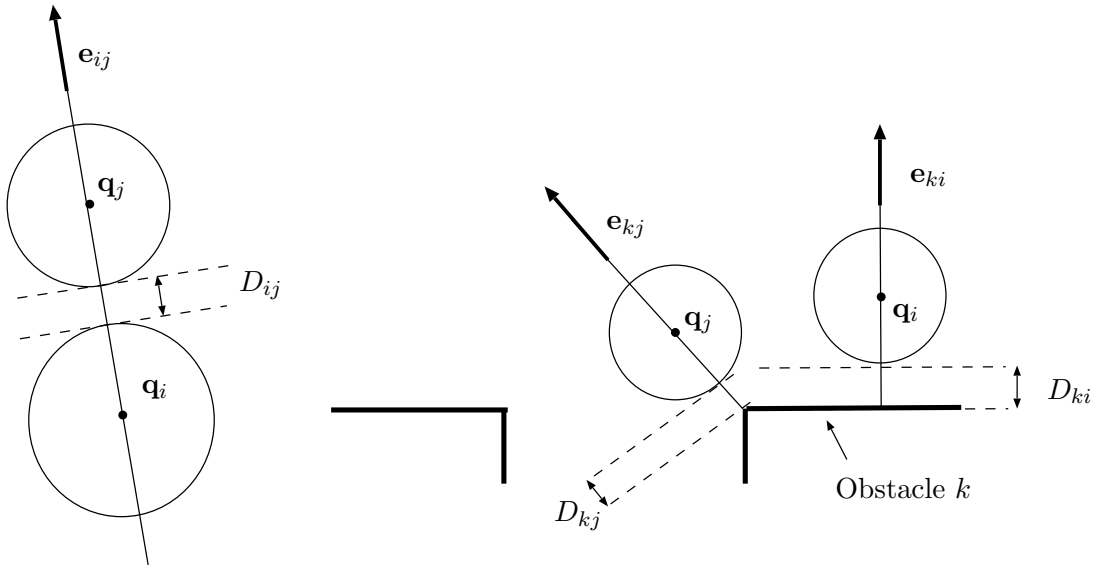

FIGURE 1. Notation for grain-grain (left) and grain-obstacle (right) interactions

where $(\alpha)_+ = \max(\alpha, 0)$ is the positive part of α, $\mathbf{G}_{ij}$ is the gradient of the distance D_{ij}:

$$\mathbf{G}_{ij} = \nabla D_{ij} = \left(0, \dots, 0, \underbrace{-\mathbf{e}_{ij}}_{i-th\text{position}}, 0, \dots, 0, \underbrace{\mathbf{e}_{ij}}_{j-th\text{position}}, 0, \dots, 0 \right).$$

with

$$\mathbf{e}_{ij} = (\mathbf{q}_j - \mathbf{q}_i) \,/\, |\mathbf{q}_j - \mathbf{q}_i| \,.$$

Note that this force automatically verifies the action-reaction law. It corresponds to a stiff repulsion force that is triggered whenever disks i and j start to overlap.

From 2^{nd} order to 1^{st} order models. A 1^{st} order model can be obtained by having τ go to 0. From a mechanical standpoint, it consists in neglecting inertial effects, and thereby replace Newton's Law (2) by an instantaneous force balance.

Proposition 1. *Let $\mathbf{q} \longmapsto \mathbf{U}(\mathbf{q})$ and $\mathbf{q} \longmapsto \mathbf{f}(\mathbf{q})$ be Lipschitzian mappings, and let $t \longmapsto \mathbf{q}_\tau(t)$ be the unique solution to*

$$\ddot{\mathbf{q}} = \frac{1}{\tau} \left(\mathbf{U}(\mathbf{q}) - \dot{\mathbf{q}} \right) + \frac{1}{\tau} \mathbf{f}(\mathbf{q}),$$

on $[0, T]$, with initial data $\mathbf{q}(0) = \mathbf{q}_0$, $\dot{\mathbf{q}}(0) = \mathbf{u}_0$. Then, when τ goes to 0, $\mathbf{q}_\tau$ uniformly converges toward $t \longmapsto \mathbf{q}(t)$ in $[0, T]$, and $\mathbf{u}_\tau = \dot{\mathbf{q}}_\tau$ uniformly converges to $\mathbf{u} = \dot{\mathbf{q}}$ on every subinterval $[\eta, T]$, with $\eta > 0$, where $\mathbf{q}$ is the unique solution to the first order differential equation

$$\dot{\mathbf{q}} = \mathbf{U}(\mathbf{q}) + \mathbf{f}(\mathbf{q}) \,, \;\; \mathbf{q}(0) = \mathbf{q}_0.$$

Proof. Without loss of generality, we consider the case $\mathbf{f} \equiv 0$ (interaction forces are merged here with forces accounting for individual tendencies). We introduce the function

$$\varphi_\tau(t) = \frac{1}{2} \left| \dot{\mathbf{q}}_\tau - \mathbf{U}(\mathbf{q}_\tau) \right|^2.$$

Its time derivative is

$$\dot\varphi_\tau = (\ddot{\mathbf{q}}_\tau - \nabla\mathbf{U}(\mathbf{q}_\tau)\cdot\dot{\mathbf{q}}_\tau)\cdot(\dot{\mathbf{q}}_\tau - \mathbf{U}(\mathbf{q}_\tau)) = -\frac{2}{\tau}\varphi_\tau - (\nabla\mathbf{U}\cdot\dot{\mathbf{q}}_\tau)\cdot(\dot{\mathbf{q}}_\tau - \mathbf{U}(\mathbf{q}_\tau))\,.$$

From the definition of φ_τ, it holds that

$$|\dot{\mathbf{q}}_\tau| \le \sqrt{2\varphi_\tau} + |U|\,,$$

which yields

$$\begin{aligned}(\nabla\mathbf{U}\cdot\dot{\mathbf{q}}_\tau)\cdot(\dot{\mathbf{q}}_\tau - \mathbf{U}(\mathbf{q}_\tau)) &\le |\nabla\mathbf{U}|\left(\sqrt{2\varphi_\tau}+|U|\right)\sqrt{2\varphi_\tau}\\ &\le \frac{1}{2}\left(\tau\,|\nabla\mathbf{U}|^2\left(\sqrt{2\varphi_\tau}+|U|\right)^2 + \frac{2\varphi_\tau}{\tau}\right)\\ &\le \tau\,|\nabla\mathbf{U}|^2\left(2\varphi_\tau + |U|^2\right) + \frac{\varphi_\tau}{\tau}.\end{aligned}$$

We finally obtain

$$\dot\varphi_\tau \le \left(2\tau\,\|\nabla\mathbf{U}\|_\infty^2 - \frac{1}{\tau}\right)\varphi_\tau + \tau\,\|\nabla\mathbf{U}\|_\infty^2\,\|\mathbf{U}\|_\infty^2\,.$$

For τ sufficiently small, the factor of φ_τ is smaller than $-1/2\tau$, so that

$$\dot\varphi_\tau \le -\frac{1}{2\tau}\varphi_\tau + C,$$

from which we deduce by a Gronwall argument that

$$0 \le \varphi_\tau(t) \le \varphi_\tau(0)e^{-t/2\tau} + 2c\tau(1-e^{-t/2\tau}).$$

We therefore have uniform convergence on $[\eta, T]$ of φ_τ toward 0, i.e. convergence of $\dot{\mathbf{q}}_\tau$ toward $\dot{\mathbf{q}}$, and uniform convergence of the trajectories $t\mapsto\mathbf{q}_\tau(t)$ toward $t\mapsto\mathbf{q}(t)$ over the whole interval $[0,T]$. Note that the convergence of velocities is uniform over the whole interval $[0,T]$ in case of well-prepared data, i.e. if $\dot{\mathbf{q}}_\tau(0) = \mathbf{u}_0 = \mathbf{U}(\mathbf{q}_0)$ (or, equivalently, $\varphi_\tau(0)=0$). In the latter situation, we have convergence of trajectories in $W^{1,\infty}(0,T)$.

□

From soft to hard models. The next step consists in hardening the contact force coefficient to obtain the nonsmooth evolution problem that will be studied and analysed in the rest of the paper. We consider the first order smooth problem, where $\mathbf{U}$ corresponds to the desired velocity, including possibly social (i.e. long distance) interaction terms, and we consider that the short range interaction factor κ writes $1/\varepsilon$:

$$\dot{\mathbf{q}}^\varepsilon = \mathbf{U}(\mathbf{q}) + \frac{1}{\varepsilon}\sum_{i\neq j}\left(r_i + r_j - \left|\mathbf{q}_j^\varepsilon - \mathbf{q}_i^\varepsilon\right|\right)_+ \mathbf{G}_{ij}(\mathbf{q}^\varepsilon). \tag{1}$$

Let us first make a *formal* asymptotic expansion of this evolution problem. When ε goes to 0, the stiff interaction forces tend to reduce, and asymptotically suppress, overlapping. The limit trajectory can be expected to lie in the set of configurations that rule out overlapping:

$$K = \left\{\mathbf{q}\in\mathbb{R}^{2N}\,,\ D_{ij}(\mathbf{q}) = |\mathbf{q}_j - \mathbf{q}_i| - r_i - r_j \ge 0 \quad \forall i\neq j\right\}.$$

Now, from (1), it holds that $\dot{\mathbf{q}}^\varepsilon - \mathbf{U}(\mathbf{q}^\varepsilon)$ can be written

$$\dot{\mathbf{q}}^\varepsilon - \mathbf{U} = \sum_{i\sim j}\lambda_{ij}\mathbf{G}_{ij}(\mathbf{q}^\varepsilon),$$

where the sum is performed over pairs of grains that overlap, and the $\lambda'_{ij}s$ (that depend on ε) are nonnegative. If we admit that this property is verified in the limit $\varepsilon \to 0$, we obtain a trajectory $t \longmapsto \mathbf{q}(t)$ contained in K, such that $\mathbf{U} - \dot{\mathbf{q}}$ is in the cone spanned by the $-\mathbf{G}'_{ij}s$ such that i and j are in contact:

$$\mathbf{U} - \dot{\mathbf{q}} \in N_{\mathbf{q}} = \left\{ -\sum_{i \neq j} \lambda_{ij} \mathbf{G}_{ij}\,,\ \lambda_{ij} \geq 0\,,\ D_{ij} > 0 \Rightarrow \lambda_{ij} = 0 \right\}.$$

As will be detailed below, this cone is the subdifferential of the indicatrix function of the feasible set K, so that $\mathbf{U} - \mathbf{q} \in N_{\mathbf{q}}$ for all times implies that

$$\mathbf{u} = P_{C_{\mathbf{q}}}(\mathbf{U})\,,$$

where $C_{\mathbf{q}}$ is the cone of feasible velocities:

$$C_{\mathbf{q}} = \left\{ \mathbf{v} \in \mathbb{R}^{2N}\,,\ D_{ij}(\mathbf{q}) = 0 \Longrightarrow \mathbf{G}_{ij}(\mathbf{q}) \cdot \mathbf{v} \geq 0 \right\}\,,\ \mathbf{G}_{ij} = \nabla D_{ij}. \tag{2}$$

First order / nonsmooth / greedy model. Let us start by rewriting properly the model that was obtained formally from the soft congestion model (1):

$$\left| \begin{array}{rcl} \mathbf{q} & = & (\mathbf{q}_1, \ldots, \mathbf{q}_N) \in \mathbb{R}^{2N}, \\ K & = & \left\{ \mathbf{q} \in \mathbb{R}^{2N}\,,\ D_{ij}(\mathbf{q}) = |\mathbf{q}_j - \mathbf{q}_i| - r_i - r_j \geq 0 \quad \forall i \neq j \right\}, \\ C_{\mathbf{q}} & = & \left\{ \mathbf{v} \in \mathbb{R}^{2N}\,,\ D_{ij}(\mathbf{q}) = 0 \Longrightarrow \mathbf{G}_{ij}(\mathbf{q}) \cdot \mathbf{v} \geq 0 \right\}\,,\ \mathbf{G}_{ij} = \nabla D_{ij}, \\ \dfrac{d\mathbf{q}}{dt} & = & P_{C_{\mathbf{q}}}(\mathbf{U}(\mathbf{q}))\,, \end{array} \right. \tag{3}$$

where $\mathbf{U} = \mathbf{U}(\mathbf{q})$ is the desired velocity field. This model was initially proposed in Refs. [30, 31], without any connection to the soft congestion model. It simply expresses that the actual velocity field $\mathbf{u} = d\mathbf{q}/dt$ is the feasible field that is the closest (in a least square sens) to the desired one $\mathbf{U}$. As detailed in Refs. [30, 31], it can be formulated as a differential inclusion [31]:

$$\frac{d\mathbf{q}}{dt} + N_{\mathbf{q}} \ni \mathbf{U}(\mathbf{q}),$$

where $N_{\mathbf{q}}$ is the so called outward normal cone to the feasible set K. This cone can be defined by polarity as the set of all those vectors that have a non-positive scalar product with feasible directions:

$$N_{\mathbf{q}} = C_{\mathbf{q}}^o = \left\{ \mathbf{v} \in \mathbb{R}^{2N}\,,\ \mathbf{v} \cdot \mathbf{w} \leq 0 \quad \forall\, \mathbf{w} \in C_{\mathbf{q}} \right\}.$$

In this setting, existence and uniqueness of a solution can be proven (see Ref. [31]). The core of the proof is the so-called *prox-regularity* of the feasible set K. We refer to Ref. [40] for a proper definition of this notion, and to Ref. [14] for the first definition of a similar notion (namely *sets with positive reach*). It means that K, defined as the intersection of complementaries of smooth convex sets, is not too far from being convex itself. In particular, the projection on K is well defined in a close neighborhood, and this property is used to build discrete solutions. This idea (called *Catching Up strategy*) has been introduced by Moreau [34] in the late 70's to handle evolution problems associated with a moving convex set in a Hilbert space, and it has been extended more recently to non convex (prox-regular) sets [43, 5].

Remark 1. *The convergence of the soft model* (1) *toward the nonsmooth one* (3) *can be proven rigorously in some cases. A similar study is proposed in Ref.* [32] *for a general class of evolution problems of the type*

$$\frac{d\mathbf{q}}{dt} \in \mathbf{U}(\mathbf{q}) - N_{\mathbf{q}},$$

where $N_{\mathbf{q}}$ *is the outward normal cone to a close prox-regular set. The problem is regularized by introducing the distance* $d_K(\cdot)$ *to the set* K*, which leads to a standard ODE problem*

$$\frac{d\mathbf{q}^\varepsilon}{dt} = \mathbf{U}(\mathbf{q}^\varepsilon) - \frac{1}{\varepsilon}\nabla d_K(\mathbf{q}^\varepsilon)^2.$$

Thanks to the prox-regularity of K*,* $\nabla d_K(\cdot)^2$ *is Lipschitz, so that* $\mathbf{q}^\varepsilon$ *is uniquely defined, and it is shown to converge to the solution of* (3)*. This exactly corresponds to the formal convergence we presented, in the case where only two-body contacts occur. In the latter situation, the sum* $\sum \left(r_i + r_j - \left|\mathbf{q}_j^\varepsilon - \mathbf{q}_i^\varepsilon\right|\right)_+^2$ *is* $d_K(\mathbf{q})^2$*, so that the last term in* (1) *is exactly the gradient of this function. For more complicated contacts, the two quantities are different, and the theory is not directly applicable.*

These well-posedness aspects are not central in the present paper, let us simply stress here that the feasible K is not convex, and that this non-convexity will play a central role in the appearance of jams (see Section 3), and the study of their stability (Section 4).

We shall now favor the *gradient flow* framework, for which we need an additional assumption on desired velocities: we assume that $\mathbf{U}$ derives from a potential Φ:

$$\mathbf{U} = -\nabla\Phi.$$

This potential can be seen as a global dissatisfaction functional that the whole crowd tends to lower, following a steepest descent strategy. A typical choice, in case of emergency evacuation, is based on the geodesic distance $D(\cdot)$ to the exit: $D(\mathbf{x})$ is the length of the shortest path from the location $\mathbf{x}$ to the closest exit door. Considering all individuals as equal contributors to the global dissatisfaction, the latter can be defined as

$$\Phi(\mathbf{q}) = \sum_{i=1}^{N} D(\mathbf{q}_i),$$

which yields

$$\mathbf{U} = \left(-\nabla D(\mathbf{q}_1), \ldots, -\nabla D(\mathbf{q}_N)\right).$$

Note that interactions between individual can be integrated to this framework, by simply adding to Φ some terms that depend on the $D'_{ij}s$. Under this assumption, the constrained evolution process can be formulated as a gradient flow for the dissatisfaction functional plus the indicatrix function of the feasible set:

$$\Psi(\mathbf{q}) = \Phi(\mathbf{q}) + I_K(\mathbf{q}) = \left| \begin{array}{ll} \displaystyle\sum_{i=1}^{N} D(\mathbf{q}_i) & \text{if} \quad \mathbf{q} \in K, \\ +\infty & \text{if} \quad \mathbf{q} \notin K. \end{array} \right. \tag{4}$$

More precisely, we may define the (Fréchet) subdifferential of Ψ as the multivalued operator

$$\mathbf{q} \longmapsto \partial\Psi(\mathbf{q}) = \left\{\mathbf{v} \in \mathbb{R}^{2N}\,,\ \Psi(\mathbf{q}) + \mathbf{v}\cdot\mathbf{h} \leq \Psi(\mathbf{q}+\mathbf{h}) + o(\mathbf{h})\right\}. \tag{5}$$

In the case of a smooth functional Ψ, this operator is single valued ($\partial\Psi(\mathbf{q}) = \{\nabla\Psi\}$), but in the present case it identifies to

$$\partial\Psi = \nabla\Phi + N_{\mathbf{q}},$$

which makes it possible to write the overall process as a generalized gradient flow:

$$\left|\begin{array}{rcl} \Psi(\mathbf{q}) & = & \displaystyle\sum_{i=1}^{N} D(\mathbf{q}_i) + I_K \quad \text{(See (4))}, \\ \dfrac{d\mathbf{q}}{dt} & \in & -\partial\Psi(\mathbf{q}), \end{array}\right. \tag{6}$$

where $\partial\Psi$ is defined by (5).

Saddle-point formulation. As stated above, the actual instantaneous velocity is the projection of the desired velocity $\mathbf{U} = -\nabla\Phi$ on the cone of feasible velocities, defined by (2). For a given configuration $\mathbf{q}$, the constraints on the velocities can be written

$$-\mathbf{G}_{ij} \cdot \mathbf{u} \leq 0 \quad \forall i \sim j,$$

where $i \sim j$ means that i and j are in contact (i.e. $D_{ij} = 0$). This can be written in matrix form $B_{\mathbf{q}}\mathbf{u} \leq 0$, where each row of $B_{\mathbf{q}}$ corresponds to an active constraint. Minimization of $|\mathbf{v} - \mathbf{U}|$ over $C_{\mathbf{q}}$ can be expressed in a saddle point manner:

$$\left|\begin{array}{lcl} \mathbf{u} + B_{\mathbf{q}}^{\star}\boldsymbol{\lambda} & = & \mathbf{U}, \\ B_{\mathbf{q}}\mathbf{u} & \leq & 0, \\ \boldsymbol{\lambda} & \geq & 0, \\ \boldsymbol{\lambda} \cdot B_{\mathbf{q}}\mathbf{u} & = & 0, \end{array}\right. \tag{7}$$

where $B_{\mathbf{q}}^{\star}$ is the transpose of $B_{\mathbf{q}}$, i.e.

$$B_{\mathbf{q}}^{\star}\boldsymbol{\lambda} = -\sum_{i\sim j} \lambda_{ij}\mathbf{G}_{ij}. \tag{8}$$

The last line of (7) is a complementary slackness condition. Since all terms of the sum have the same sign, each one of them is zero, i.e. $\lambda_{ij}\,\mathbf{G}_{ij}(\mathbf{q}) \cdot \mathbf{u} = 0$. Note that, if we consider active constraints only (i.e. for which $\lambda_{ij} > 0$), the latter identity implies that $B_{\mathbf{q}}\mathbf{u} = 0$ (we keep the same notation $B_{\mathbf{q}}$ for the matrix expressing active constraints). Since $\mathbf{u} = \mathbf{U} - B_{\mathbf{q}}^{\star}\boldsymbol{\lambda}$, we obtain

$$B_{\mathbf{q}}B_{\mathbf{q}}^{\star}\boldsymbol{\lambda} = B_{\mathbf{q}}^{\star}\mathbf{U}. \tag{9}$$

Since $B_{\mathbf{q}}$ can be seen as a discrete version of the opposite of the divergence operator, and $B_{\mathbf{q}}^{\star}$ the discrete counterpart of the gradient operator, Eq. (9) can be interpreted formally as a discrete Poisson problem for the "pressure field" $\boldsymbol{\lambda}$. For a one-dimensional problem, with N individuals in a thin corridor, in contact with each other, $B_{\mathbf{q}}B_{\mathbf{q}}^{\star}$ is indeed the discrete Laplacian matrix [25]. Let us stress, though, that in the general case of discs in a two dimensional domain, this matrix does not qualify as a discrete Laplacian, in particular it does not verify the maximum principle (see next section).

Numerical aspects. Problem (3) can be discretized in time by linearizing the constraints [31, 45]. The idea is borrowed from granular flow simulations [26]: we denote by $\mathbf{q}^n$ the position vector at time t^n. The next position vector is $\mathbf{q}^{n+1} = \mathbf{q}^n + \tau \mathbf{u}^{n+1}$, where $\tau = t^{n+1} - t^n > 0$ is the time step. We replace the requirement $D_{ij}(\mathbf{q}^{n+1}) \geq 0$ by its first order asymptotic expansion:

$$D_{ij}(\mathbf{q}^{n+1}) \approx D_{ij}(\mathbf{q}^n) + \tau \mathbf{G}_{ij}(\mathbf{q}^n) \cdot \mathbf{u}^{n+1} \geq 0.$$

The discretization scheme consists in computing the next velocity $\mathbf{u}^{n+1}$ as

$$\mathbf{u}^{n+1} = \arg\min_{\mathbf{v} \in C^n} \frac{1}{2} \left| \mathbf{v} - \mathbf{U}(\mathbf{q}^n) \right|^2,$$

where C^n is the discrete set of feasible velocities

$$C^n = \left\{ \mathbf{v} \in \mathbb{R}^{2N}, \ D_{ij}(\mathbf{q}^n) + \tau \mathbf{G}_{ij}(\mathbf{q}^n) \cdot \mathbf{v} \geq 0 \quad \forall i \neq j \right\}$$

The latter is a closed convex set, that is included in $C_{\mathbf{q}^n}$ (defined by the third equation of (3)). The projection is computed by using a Uzawa algorithm on the saddle-point formulation of this contrained minimization problem. We refer again to Ref. [31] for details on implementation aspects, and to Ref. [45] for a proof of convergence of this algorithm.

3. Static jams

The notion of jams is not clearly defined in a crowd motion context. It can be defined as a situation such that velocities are almost zero during some time [24]. We shall make here the distinction between these transitory jams and what we will call *static* jams, also called *blocking clusters* in Ref. [36]. The latter are somewhat academic in nature, since real jams usually break after some time. Yet, some have been reported to be very stable in extreme situations, and we shall see that their study sheds light on the evacuation process. From a gradient flow standpoint, jams correspond to steady solutions, i.e. configurations $\mathbf{q}$ such that

$$0 \in \partial \Psi(\mathbf{q}),$$

or, equivalently,

$$\mathbf{U} + \sum_{i \sim j} \lambda_{ij} \mathbf{G}_{ij}(\mathbf{q}) = 0, \tag{10}$$

for some Lagrange multiplier field $\boldsymbol{\lambda} = (\lambda_{ij}) \in \mathbb{R}_+^{N_c}$, where N_c is the number of active contacts. Let us illustrate such a situation by an example. Fig. 2 represents a 15-people jam: contact network (top) and force balance (bottom). The bottom figure graphically expresses Eq. (10). The bold arrows represent, for each individual, the desired velocity $\mathbf{U}_i$, whereas thin arrows account for contact forces. For each individual, this contribution is

$$\left(\sum_{i \sim j} \mathbf{G}_{ij}(\mathbf{q}) \right)_i = - \sum_{i \sim j} \lambda_{ij} \mathbf{e}_{ij}.$$

From (9), it corresponds to a pressure field $\boldsymbol{\lambda}$ that is *harmonic* in some sense, since we have

$$B_{\mathbf{q}} B_{\mathbf{q}}^\star \boldsymbol{\lambda} = B_{\mathbf{q}}^\star \mathbf{U}.$$

The matrix $B_{\mathbf{q}} B_{\mathbf{q}}^\star$ is a Laplacian-like operator associated to the network that is *dual* to the contact network (Fig. 2, top). The vertices of this dual network are the edges of the primal one, it is represented in Fig. 2 (middle). As previously mentioned, $B_{\mathbf{q}} B_{\mathbf{q}}^\star$ is not

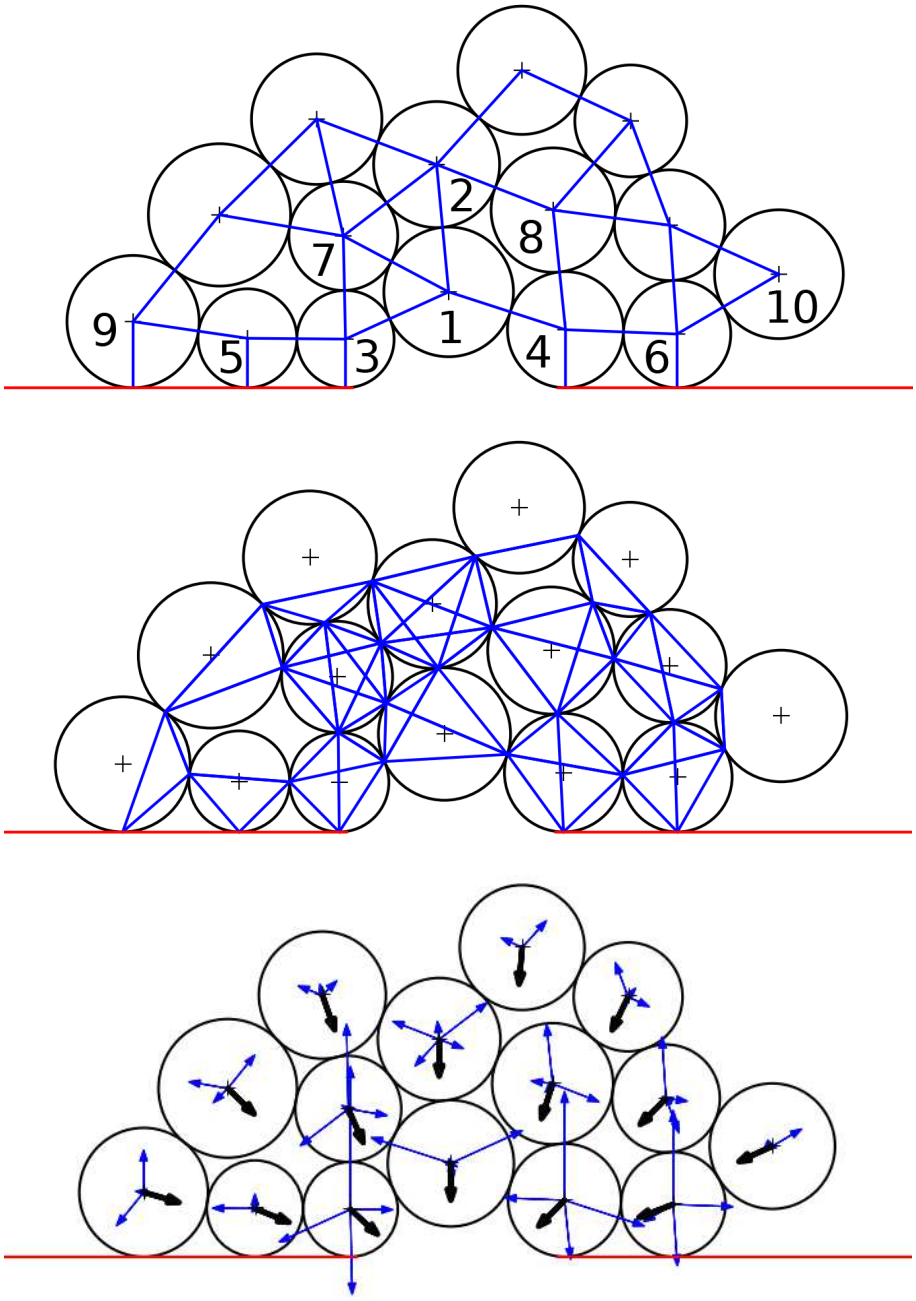

FIGURE 2. Contact network (top), dual graph (middle), and force balance (bottom), for a static jam

a discrete Laplacian in a standard sense. In particular, it is not a Z–matrix: whereas diagonal entries are positive, some extra-diagonal entries may also be positive, which rules out the maximum principle.

This example sheds light on phenomena usually referred to as *arches*. Consider the two individual facing the door. The one that is the closest to the exit, i.e. disk 1, is maintained

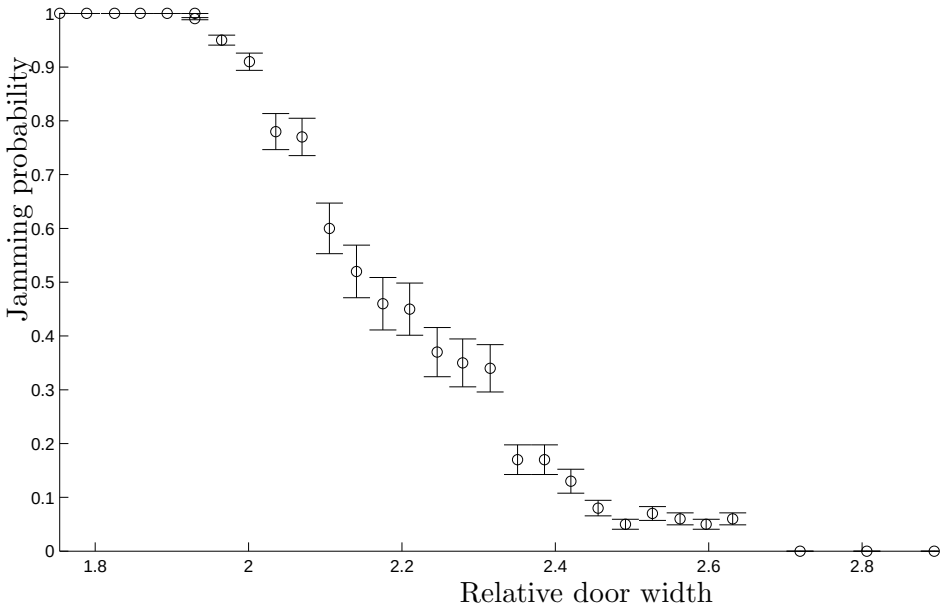

FIGURE 3. Jamming probability *vs.* relative door width

static by forces exerted from individuals that are on his side (3 and 4). Considering the angle of contact (the three disks at the door are almost aligned) this calls for a contact force with an important horizontal component, much higher than individual forces. This is made possible by the action of other individuals that play the role of butresses (*contreforts* in french), namely 5, 6, 9 and 10. The situation of disc 2 is also interesting. There is almost no interaction with 1, its desired velocity is counteracted by side neighbors 7 and 8, which are themselves maintained by 3 and 4, respectively. We therefore have two *arches*: a 3-people one next to the door, $3-1-4$, and a wider one $3-7-2-8-4$, both arches being reinforced by individuals on the side (5 and 9 and the left, 6 and 10 on the right).

Such jams are obviously more likely to occur when the door is small compared to individual sizes. To investigate this more precisely, we consider the following situation: $N = 200$ individuals are disposed randomly in a square room, with slightly polydisperse radii:

$$r_i = r \pm 5\,\%,$$

All individuals head to the unique exit door, the size of which is L. Following a Monte Carlo approach, we evaluate the probablity of a static jam to occur, for different values of L. For each value of $L/(2r)$ (relative width of the door with respect to the mean individual diameter), we run 100 computations associated to randomly chosen initial data, and we plot the estimated jamming probablility (see Fig. 3).

The figure exhibits a transition zone that corresponds to door widths for which jams may happen, but they are not systematic. For smaller doors (relative width smaller than 2), evacuation never gets to its end, whereas above a value of 2.7, jams never happen.

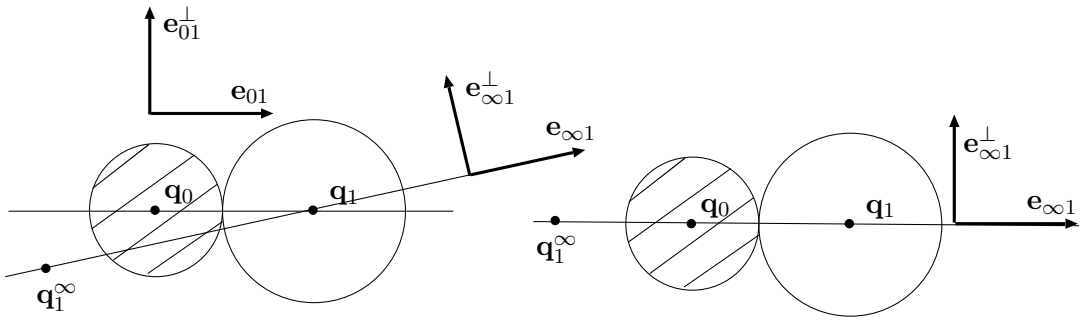

FIGURE 4. Notation for the two-grain toy problem

4. Stability issues

This section addresses the question of the stability of jams. We shall first propose a new approach to assess stability of computed (or observed) jams. This semi-heuristic approach is based on a full stability analysis of the regularized problem, for which hard contact is relaxed and replaced by stiff forces that penalize overlapping between particles.

4.1. **A two-grain toy problem.** In order to describe the approach, we start with a very simple example with only two degrees of freedom. We consider the situation represented in Fig. 4: the particle 0 (shaded disc) is assumed to be fixed, and particle 1 tends to minimize the distance of its center to a fixed point $\mathbf{q}_1^{\infty}$, under the non-overlapping constraint

$$|\mathbf{q}_1 - \mathbf{q}_0| \geq r_0 + r_1.$$

The corresponding gradient flow writes

$$\frac{d\mathbf{q}_1}{dt} \in -\partial\Psi_0(\mathbf{q}_1)\,, \qquad \text{with } \Psi_0(\mathbf{q}_1) = |\mathbf{q}_1 - \mathbf{q}_1^{\infty}| + I_K(\mathbf{q}_1).$$

The desired velocity is $\mathbf{U} = -\nabla\,|\mathbf{q}_1 - \mathbf{q}_1^{\infty}| = -\mathbf{e}_{\infty 1}$. Obviously, the situation represented on the right of Fig. 4 is a fixed point as soon as $\mathbf{q}_{\infty 1}$ lies on the line $(\mathbf{q}_0, \mathbf{q}_1)$, on the left of $\mathbf{q}_1$. The equilibrium writes more formally

$$0 \in -\partial\left(|\mathbf{q}_1 - \mathbf{q}_1^{\infty}| + I_K(\mathbf{q}_1)\right) \Longleftrightarrow -\mathbf{e}_{\infty 1} + \lambda \mathbf{e}_{01} = 0,$$

where $\lambda \geq 0$ is the Lagrange multiplier, that is obviously equal to 1 in the present situation. Regarding the stability of this fixed point, it is natural to expect the fixed point to be stable as soon as $\mathbf{q}_{\infty 1}$ is closer to $\mathbf{q}_1$ than $\mathbf{q}_0$. The question can be investigated by introducing the relaxed gradient flow associated to the functional

$$\Psi_\varepsilon(\mathbf{q}_1) = |\mathbf{q}_1 - \mathbf{q}_1^{\infty}| + \frac{1}{2\varepsilon}\left(r_0 + r_1 - |\mathbf{q}_1 - \mathbf{q}_0|\right)_+^2,$$

where $(\alpha)_+ = \max(0, \alpha)$ stands for the *positive* part of α. Whenever there is overlapping, the gradient of Ψ_ε is

$$\nabla\Psi_\varepsilon = \mathbf{e}_{\infty 1} - \frac{1}{\varepsilon}\left(r_0 + r_1 - |\mathbf{q}_1 - \mathbf{q}_0|\right)\mathbf{e}_{01}.$$

Therefore equilibrium for this relaxed problem writes

$$\mathbf{e}_{\infty 1} - \frac{1}{\varepsilon}\left(r_0 + r_1 - |\mathbf{q}_1 - \mathbf{q}_0|\right)\mathbf{e}_{01} = 0.$$

This equilibrium is characterized by a small overlap between grains, the size of which is ε (in order to fulfill the equilibrium equation above). The Hessian matrix is

$$\begin{aligned} H_\varepsilon = \nabla^2 \Psi_\varepsilon &= \frac{1}{|\mathbf{q}_1 - \mathbf{q}_1^\infty|} \mathbf{e}_{\infty 1}^\perp \otimes \mathbf{e}_{\infty 1}^\perp \\ &\quad - \frac{1}{\varepsilon} \frac{1}{|\mathbf{q}_1 - \mathbf{q}_0|} \left(r_0 + r_1 - |\mathbf{q}_1 - \mathbf{q}_0| \right) \mathbf{e}_{01}^\perp \otimes \mathbf{e}_{01}^\perp \\ &\quad + \frac{1}{\varepsilon} \mathbf{e}_{01} \otimes \mathbf{e}_{01} \\ &= H_\infty + H_\lambda + \frac{1}{\varepsilon} H_S. \end{aligned}$$

Thanks to the equilibrium relation, the second contribution writes

$$H_\lambda = - \frac{\lambda}{|\mathbf{q}_1 - \mathbf{q}_0|} \mathbf{e}_{01}^\perp \otimes \mathbf{e}_{01}^\perp \quad \text{with } \lambda = 1.$$

Its non-positive character reflects the non-convexity of the feasible set K. Stability is ensured as soon as the eigenvalues of H_ε are positive. Since the relaxed problem tends to the non-smooth one, stability of the non-smooth problem depends on whether the eigenvalues of H_ε remain positive and bounded away from 0. Now, since H_S (the letter S stands for *stiffness*) is nonnegative, for any vector v that does not lie in the kernel of H_S, we have

$$\frac{1}{\varepsilon} \left(H_S v, v \right) \longrightarrow + \infty \Longrightarrow \left(H_\varepsilon v, v \right) \longrightarrow + \infty.$$

It is therefore sufficient to check that the bilinear form associated to $H_\infty + H_\lambda$, restricted to the kernel of H_S, has positive eigenvalues. Let us denote by $H^\star$ the corresponding matrix (it is actually a 1×1 matrix in this simple example). The kernel of H_S is $\mathbb{R} \mathbf{e}_{01}^\perp$, so that

$$H^\star = \frac{1}{|\mathbf{q}_1 - \mathbf{q}_1^\infty|} - \frac{1}{|\mathbf{q}_1 - \mathbf{q}_0|}.$$

It is indeed positive if and only if $|\mathbf{q}_1 - \mathbf{q}_1^\infty| < |\mathbf{q}_1 - \mathbf{q}_0|$, that is the expected stability condition.

4.2. **Stability criterium for the many-body problem.** We propose a straight extension of this approach to the many-body problem, to the expense of some unavoidable complexity in terms of notation. We now consider an $N-$ body gradient flow for

$$\mathbf{q} = \left(\mathbf{q}_1, \dots, \mathbf{q}_N \right),$$

corresponding to the following functional:

$$\Psi(\mathbf{q}) = \sum_{i=1}^N |\mathbf{q}_i - \mathbf{q}_{\infty i}| + I_K(\mathbf{q}), \tag{11}$$

where I_K stands for the indicator function of the feasible set

$$K = \left\{ \mathbf{q} \in \mathbb{R}^{2N}, \ |\mathbf{q}_j - \mathbf{q}_i| - r_i - r_j \geq 0 \quad \forall\, i \neq j \right\}.$$

Although not explicitely written (to alleviate notation), we shall consider that grain-wall interactions are also contained in K.

Remark 2. *The formulation above presents a difference with the original model: whereas the individual dissatisfaction was $D(\mathbf{q}_i)$, we replaced in* (11) *this expression by $|\mathbf{q}_i - \mathbf{q}_{\infty i}|$. This modification is due to the fact that the second derivative of this dissatisfaction will be involved in the stability study, and the new form will make it possible to explicitly compute*

the Hessian. Let us explain more explicitly the link between the two expressions, in the case of a square room with a single exit door. In the zone that faces the door, everybody points to the door, the dissatisfaction function is affine, and its gradient is orthogonal to the door. In this case, we shall consider that the objective point is at infinity, so that $1/|\mathbf{q}_i - \mathbf{q}_{\infty i}| = 0$*, which simply means that the Hessian of* D *vanishes uniformly in this zone. For people on the sides, the dissatisfaction* $D(\mathbf{q}_i)$ *is* $|\mathbf{q}_i - \mathbf{q}_\infty|$*, where* $\mathbf{q}_\infty$ *is the endpoint of the door that is the closest. Isolines of the dissatisfaction are circles in these zones, and the curvature (that is also the non-zero eigenvalue of the Hessian matrix) is the reciprocal of the radius, i.e.* $1/|\mathbf{q}_i - \mathbf{q}_{\infty i}|$*.*

The evolution problem writes

$$\frac{d\mathbf{q}}{dt} + \partial I_K(\mathbf{q}) \ni \mathbf{U}\,, \quad \text{with } \mathbf{U} = -\nabla\left(\sum_{i=1}^{N} |\mathbf{q}_i - \mathbf{q}_{\infty i}|\right). \tag{12}$$

In order to express $2N$-vectors and $2N \times 2N$ matrices in a concise way, we shall use the following convention: for any vector $\mathbf{v} \in \mathbb{R}^2$, any i between 1 and N, we set

$$\mathbf{v}^i = \left(0, 0, \ldots, 0, \underbrace{\mathbf{v}^T}_{i-th \text{ position}}, 0, \ldots, 0\right)^T.$$

Under this convention, the gradient $\mathbf{G}_{ij}$ of

$$D_{ij} = |\mathbf{q}_j - \mathbf{q}_i| - r_i - r_j$$

can be expressed as

$$\mathbf{G}_{ij} = \mathbf{e}_{ij}^j - \mathbf{e}_{ij}^i.$$

Accordingly, since $\mathbf{U}_i = -\mathbf{e}_{\infty i} \in \mathbb{R}^2$, it holds

$$\mathbf{U} = \sum_{i=1}^{N} -\mathbf{e}_{\infty i}^i \in \mathbb{R}^{2N}.$$

A static solution $\mathbf{q}$ of the gradient flow (static jam) is characterized by

$$0 \in \partial\Psi(\mathbf{q}),$$

which can be written

$$\mathbf{U} + \sum_{i\sim j} \lambda_{ij}\mathbf{G}_{ij} = 0\,,$$

or, equivalently,

$$\sum_{i=1}^{N} \mathbf{e}_{\infty i}^i - \sum_{j\sim i} \lambda_{ij}(\mathbf{e}_{ij}^j - \mathbf{e}_{ij}^i) = 0, \tag{13}$$

where the $\lambda_{ij}'s$ are the Lagrange multipliers, which are nonnegative and verify the complementary slackness condition

$$\lambda_{ij}(|\mathbf{q}_j - \mathbf{q}_i| - r_i - r_j) = 0.$$

The relaxed (or penalized) problem is the gradient flow associated to the functional

$$\Psi_\varepsilon(\mathbf{q}) = \sum_{i=1}^{N} |\mathbf{q}_i - \mathbf{q}_{\infty i}| + \frac{1}{2\varepsilon}\sum_{i\neq j}(r_i + r_j - |\mathbf{q}_j - \mathbf{q}_i|)_+^2.$$

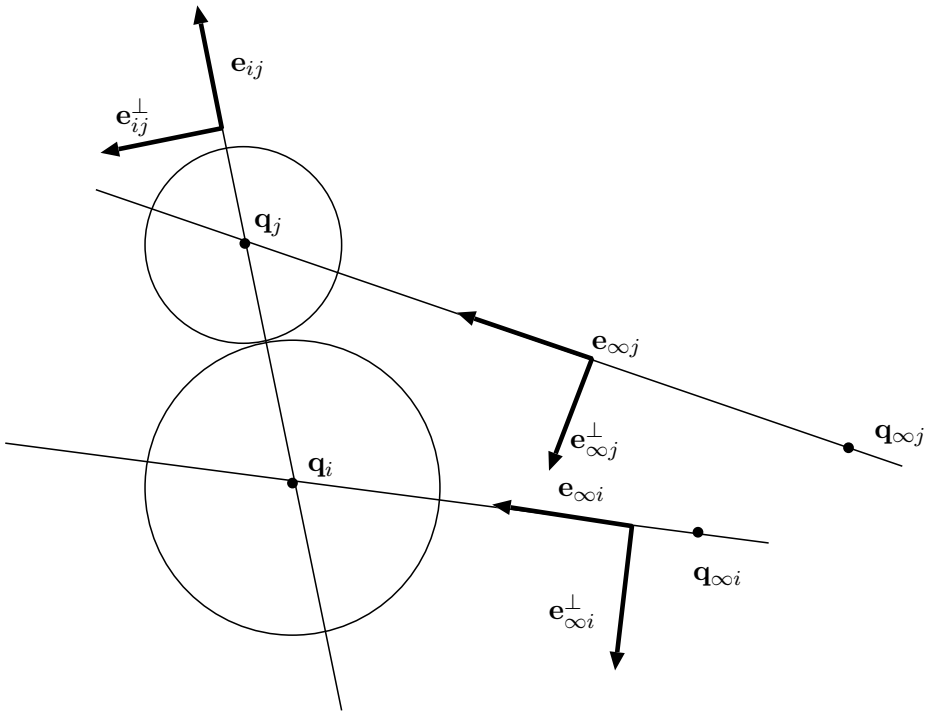

FIGURE 5. Notation for the interaction between grains i and j

A static solution for this gradient flow is characterized by

$$\nabla\Psi_\varepsilon = 0 \Longleftrightarrow \sum_{i=1}^{N} \mathbf{e}_{\infty i}^{i} - \frac{1}{\varepsilon}\sum_{i\sim j}(|\mathbf{q}_j - \mathbf{q}_i| - r_i - r_j)(\mathbf{e}_{ij}^{j} - \mathbf{e}_{ij}^{i}) = 0, \tag{14}$$

where $i \sim j$ means that i and j are in active contact, i.e. the two disks overlap ($D_{ij} < 0$). For ε small enough, we shall have $|\mathbf{q}_j - \mathbf{q}_i|$ close to 0, and the penalty term in (14) identifies to the Lagrange multiplier in (13):

$$\lambda_{ij} \approx \frac{1}{\varepsilon}(|\mathbf{q}_j - \mathbf{q}_i| - r_i - r_j).$$

The Hessian matrix associated to the penalized problem can be expressed (see A), like in the one-grain situation, as the sum of three contributions :

$$\begin{aligned} H_\varepsilon = \nabla^2\Psi_\varepsilon \;=\; & \sum_i \frac{1}{|\mathbf{q}_i - \mathbf{q}_i^\infty|}\mathbf{e}_{\infty i}^{\perp}\otimes\mathbf{e}_{\infty i}^{\perp} \\ & - \sum_{i\sim j}\frac{\lambda_{ij}}{|\mathbf{q}_j - \mathbf{q}_i|}\left(\mathbf{e}_{ij}^{\perp i}\otimes\mathbf{e}_{ij}^{\perp i} + \mathbf{e}_{ij}^{\perp j}\otimes\mathbf{e}_{ij}^{\perp j} - \mathbf{e}_{ij}^{\perp i}\otimes\mathbf{e}_{ij}^{\perp j} - \mathbf{e}_{ij}^{\perp j}\otimes\mathbf{e}_{ij}^{\perp i}\right) \\ & + \frac{1}{\varepsilon}\sum_{i\sim j}\left(\mathbf{e}_{ij}^{i}\otimes\mathbf{e}_{ij}^{i} + \mathbf{e}_{ij}^{j}\otimes\mathbf{e}_{ij}^{j} - \mathbf{e}_{ij}^{i}\otimes\mathbf{e}_{ij}^{j} - \mathbf{e}_{ij}^{j}\otimes\mathbf{e}_{ij}^{i}\right) \\ & = H_\infty + H_\lambda + \frac{1}{\varepsilon}H_S. \end{aligned} \tag{15}$$

The first term, H_∞, is the Hessian of the global dissatisfaction function. Since, in our case, each individual tends to reach a certain objective, this function is convex, which is

reflected by the semi-positivity of H_∞. Note that it is degenerate: The rank of H_∞ is less or equal to N (some eigenvalues might vanish if the objective point is at infinity), whereas it is a $2N \times 2N$ matrix.

The third term H_S, that is penalized by $1/\varepsilon$, corresponds to a stiffness matrix. It penalized changes in interparticle distances for particles that are already in contact. It can be written as $B_{\mathbf{q}}^\star B_{\mathbf{q}}$, where $B_{\mathbf{q}}$ is the matrix each line of which expresses the distance gradient (see Eq. (8)). It is a semi-definite positive matrix. The kernel of H_S contains elementary displacement fields that do not change distances at the first order. It contains in particular rigid motions, but it can be richer in looser situations.

The second term H_λ is the potential source of negative eigenvalues (and thereby a source of instability), it encodes the curvatures of the non-overlapping constraints. Its non-positive characters expresses the non convexity of the feasible set K (defined as the intersection of the *complementaries* of convex sets).

The stability issue can be interpreted as a competition between these three terms (1 and 3 against 2): stiffness of the assemby and individual tendencies provide stability (i.e. they push the global Hessian toward the positive direction), while sliding motions between individuals in contact tend to destabilize clusters.

Remark 3. *Let us stress that the crowd motion situation is more likely to create static jams than the standard situation of grains under the action of gravity. In the latter situation, the "desired velocity" is replaced by a uniform downward force. It corresponds to the situation of people heading to a straight line (see Remark 2), i.e. with a objective at infinite. This does not create any positive eigenvalue, since the Hessian of the underlying function is zero. On the other hand, for people pointing toward a point $\mathbf{q}_\infty$ at finite distance, the associated function $|\cdot - \mathbf{q}_\infty|$ is strictly convex in some directions, thereby increasing the overall convexity of the global functional, thus increasing the likehood of having stable local minima.*

Like in the one-grain situation, a simple stability criterium can be deduced (at least formally) from these considerations, by having ε go to 0.

Definition 1. *Let* $\mathbf{q}$ *be a static solution of* (12)*, i.e. such that* (13) *holds. Let H_∞, H_S, and H_λ be the symmetic matrices defined by*

$$H_\infty = \sum_i \frac{1}{|\mathbf{q}_i - \mathbf{q}_i^\infty|} \mathbf{e}_{\infty i}^\perp \otimes \mathbf{e}_{\infty i}^\perp \,,$$

$$H_S = \sum_{i\sim j} \left(\mathbf{e}_{ij}^i \otimes \mathbf{e}_{ij}^i + \mathbf{e}_{ij}^j \otimes \mathbf{e}_{ij}^j - \mathbf{e}_{ij}^i \otimes \mathbf{e}_{ij}^j - \mathbf{e}_{ij}^j \otimes \mathbf{e}_{ij}^i \right)$$

$$H_\lambda = -\sum_{i\sim j} \frac{\lambda_{ij}}{|\mathbf{q}_j - \mathbf{q}_i|} \left(\mathbf{e}_{ij}^{\perp i} \otimes \mathbf{e}_{ij}^{\perp i} + \mathbf{e}_{ij}^{\perp j} \otimes \mathbf{e}_{ij}^{\perp j} - \mathbf{e}_{ij}^{\perp i} \otimes \mathbf{e}_{ij}^{\perp j} - \mathbf{e}_{ij}^{\perp j} \otimes \mathbf{e}_{ij}^{\perp i} \right).$$

Let $H^\star$ be the matrix that expresses the restriction to the kernel of H_S of the quadratic form associated to $H_\infty + H_\lambda$. Then $\mathbf{q}$ is stable whenever all eigenvalues of $H^\star$ are positive.

Before applying this criterium to static jams let us make some remarks:

Remark 4. *If the kernel of H_S is "small" (i.e. of dimension* 0 *or* 1*), stability will be straightforwardly obtained, as soon a the dissatisfaction contribution H_∞ provides any convexity in the direction of the kernel. In the case of* loosely jammed *configurations, the dimension of the kernel might be larger, increasing the instability likelyhood. In this kernel, the stability* vs. *instability competition occurs between H_∞ (positive semi-definite) and*

H_λ (negative semi-definite). Now the eigenvalues of H_∞ correspond to the dissatisfaction curvatures: $1/|\mathbf{q}_i - \mathbf{q}_i^\infty|$*, where $\mathbf{q}_i^\infty$ is the objective of individual i. On the other hand, the eigenvalues of the contributions of H_λ (one contribution for each contact) are the opposite of the constraint curvatures, i.e* $1/|\mathbf{q}_i - \mathbf{q}_j|$*. Unless an individual tends to reach a point that is* inside *one of his neighbor, the distance of an individual to its objective is in general much larger than the typical size of individuals. As a consequence, the second contributions are much larger in general. Therefore it can be expected that, if the looseness of the configuration is sufficient (i.e. the kernel of H_S contains non trivial fields), instability should prevail in general.*

Remark 5. *Following the previous remark, let us add that negative eigenvalues of $H^\star$ quantify the instability. Unstable static jams correspond to saddle points of the global (i.e. uncluding the constraints) dissatisfaction functional. Thus, very negative eigenvalue correspond to very unstable jams, so that the time taken by the crowd to exit the saddle-point and recover some fluidity will be smaller than in the case of negative eigenvalues that are close to* 0*. This remark will be illustrated in the next section (see Fig. 7 and comments thereof).*

4.3. **Stability study of jams.** The stability criterium that has been proposed can be applied to evalute the stability of jams that are encountered in the simulations. The first observation that can be made is consistent with Remark 4: All static jams that are observed in numerical computations correspond to configurations for which the dimension of the kernel of H_S is 1. In the evacuation situation we consider, this kernel corresponds to a translational motion parallel to the wall. Fig. 8 represents such a jammed configuration.

We shall now illustrate in an example how this stability analysis sheds a light on the way evacuation proceeds. In order to quantify and graphically represent the fluidity of the evacuation process, we propose to focuse on a notion that we define as the *mean frustration*, in the following way: For an individual i, with desired velocity $\mathbf{U}_i$ and actual velocity $\mathbf{u}_i$, we define its instantaneous frustration as

$$f_i = 1 - \frac{\mathbf{u}_i \cdot \mathbf{U}_i}{|\mathbf{U}_i|^2}. \tag{16}$$

It is a dimensionless quantity, equal to 0 when i achieves its desired velocity, and to 1 when $\mathbf{u}_i$ is 0, or orthogonal to the desired direction. Note that, in the case where $\mathbf{U}_i = -\nabla D(\mathbf{q}_i)$, where $D(\mathbf{q}_i)$ is the distance to the exit (individual dissatisfaction), it holds that $|\mathbf{U}_i| = 1$, and

$$\frac{d}{dt} D(\mathbf{q}_i(t)) = \nabla D \cdot \frac{d\mathbf{q}_i}{dt} = -\mathbf{u}_i \cdot \mathbf{U}_i = -\frac{\mathbf{u}_i \cdot \mathbf{U}_i}{|\mathbf{U}_i|^2} = f_i - 1.$$

Therefore the frustration f_i is equal to 1 (or larger) as soon as i is not currently reducing its dissatisfaction. We define the global mean frustration as

$$F = \frac{1}{N_{int}} \sum_{I_{int}} f_i, \tag{17}$$

where the sum is performed over all individuals who are still in the room. Note that, according to the previous considerations, it holds that

$$F = 1 + \frac{1}{N_{int}} \frac{d\Phi}{dt}, \quad \text{with } \Phi = \sum_{I_{int}} D(\mathbf{q}_i).$$

It is the curvature of the iso-dissatisfaction curve, that is a circle in this situation.

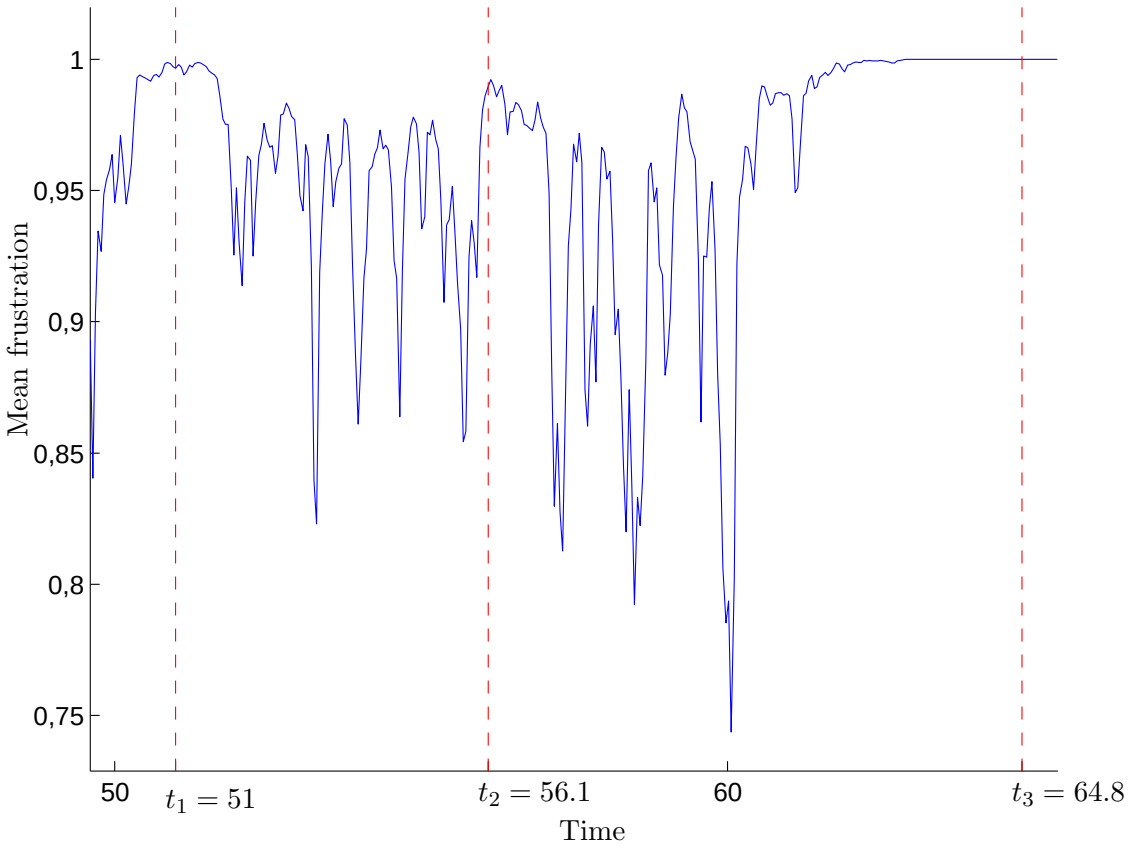

FIGURE 6. Evolution of the frustration during evacuation

The global frustration F therefore quantifies at which rate the global dissatisfaction decreases.

We consider again the evacuation of a square room, with a unique door. The number of individuals initially in the room is 500. Figure 6 plots the mean frustration between times 50 and 64. The alternation of plateaus where F is close to 1, and stiff decreases to a smaller value illustrates the Stop and Go waves phenomenon.

These plateaus corresponds to unstable jams. The vector $\mathbf{q}$ is in the neighborhood of a critical point of the functional Ψ, i.e. a point at which 0 lies in the subdifferential $\partial\Psi$, for which the corresponding jam is unstable according to definition 1. Indeed, at $t_1 = 51$, the mean frustration is 0.997 (quasi-static situation), the dimension of $\ker H_S$ is 10, and the smallest eigenvalue of $H^\star$ is -21.3. Similarly, at $t_2 = 56.1$, the mean frustration is 0.990, the dimension of $\ker H_S$ is 18, and the smallest eigenvalue of $H^\star$ is -18.8.

In both cases, the cluster slowly destabilizes along the direction that corresponds to the eigenvector associated to the smallest eigenvalue of $H^\star$. To illustrate this point, we plotted in Fig. 7 the actual velocity field at time t_1 (top), and the eigenvector of matrix $H^\star$ associated to its smallest eigenvalue, at the same time. The similarity between both fields strongly suggests that the actual evolution process is indeed controlled by the Hessian matrix in the neighborhood of the critical point.

Then the cluster abruptly crumbles (it corresponds to downward peaks in Fig.6), untill it reaches the next quasi-flat zone of the dissatisfaction function.

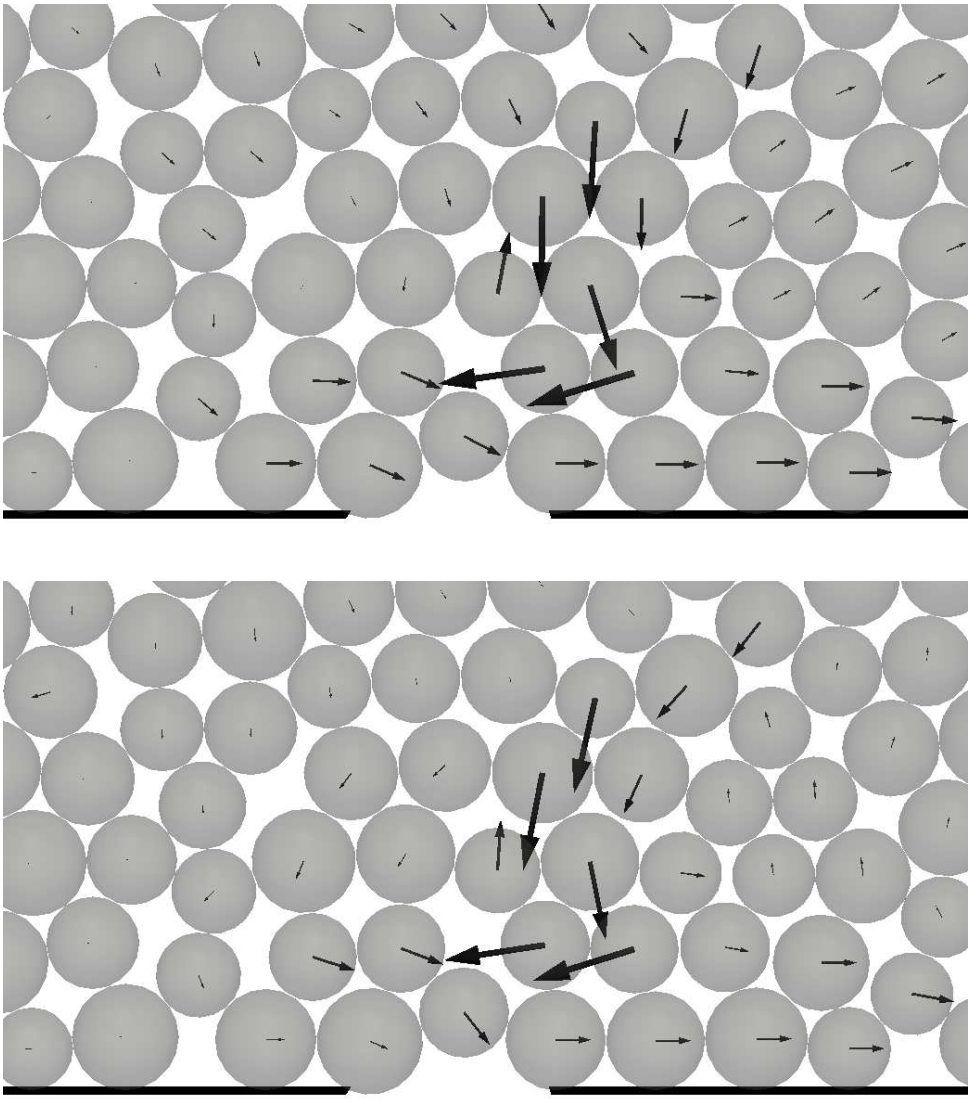

FIGURE 7. Velocity field (top) and first eigenvector of $H^\star$ (bottom)

At the end of the time interval, the frustration goes up to 1 and stabilizes: a static jam is reached (see Fig. 8). At time $t_3 = 64.8$, the mean frustration is exactly 1, the kernel of H_S is one-dimensional, and the associated eigenvalue is 0.07, which asserts the stability of the jam.

5. Active breaking of static jams and "slower is faster" effect

In this exploratory section we investigate the possibility to define strategies in order to fluidize the evacuation process, on the basis of the previous developments. Let us first remark that the underlying control problem is quite poor, if no assumption is made on the way one aims at controling the crowd. More precisely, considering an initial configuration, the general problem may be formulated as follows: Find velocities $\mathbf{u}_1, \ldots, \mathbf{u}_N$, under the

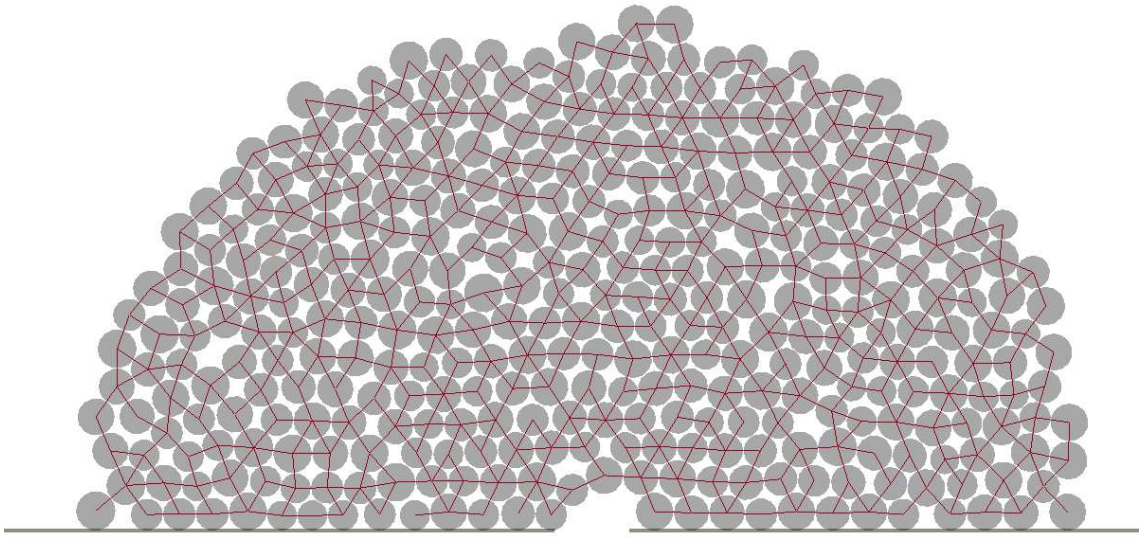

FIGURE 8. Example of a 363-people stable jam

constraint that $|\mathbf{u}_i|$ is less than a prescribed maximal velocity, such that the associated trajectory $t \mapsto \mathbf{q}(t)$ lies in K (no overlapping is allowed), and such that the evacuation process is optimal in some sense. If one aims for instance at minimizing the evacuation time of the last individual to exit, the actual problem may raise technical and mathematical difficulties, but its practical relevance is quite limited. Indeed, it is straightforward to heuristically build reasonably optimal strategies, by taking care of individuals one after another, starting with those that are the closest to the door, and sometimes choosing arbitrarily between two of them which one will exit first. Such a strategy makes sense in some very particular contexts, like the case of perfectly obeying soldiers controled by an almighty supervisor, but it is ruled out in general evacuation processes under panic.

In order to account for the practical impossibility to control all individuals with a full and global knowledge of the configuration, we propose a new framework that is compatible with the greedy character of the evolution process, and with the fact that each individual is able to observe the crowd in its close neighborhood only. In this spirit, we assume that any individual may only change his desired behavior by "taking on himself", namely reducing the weight of its own dissatisfaction in the global dissatisfaction function, without knowledge of the positions of other people except for those that are in its close neighborhood. The approach that is detailed below aims at recovering the effect that is commonly referred to as "faster is slower" in the literature [19, 36]. Actually, we shall illustrate the reverse phenomenon, by showing that a *decrease* of the desired speed of some individuals can improve the fluidity of the evacution process, i.e. *increase* the overall evacuation speed.

The framework we propose here is based on a global dissatisfaction function modified by *taking on one's self* parameters $\beta_i \in [0, 1]$, a smaller β_i meaning that individual i accepts to momentarily inhibit its will to reach its goal. Consider the case were the dissatisfaction

of an individual at $\mathbf{q}_i$ writes $D(\mathbf{q}_i)$, that is typically the distance to the exit of $\mathbf{q}_i$, we define the instantaneous dissatisfaction functional as

$$\Phi_\beta(\mathbf{q}) = \sum_{i=1}^{N} \beta_i D(\mathbf{q}_i),$$

and we assume that the actual velocity field is the projection of

$$-\nabla\Phi_\beta(\mathbf{q}) = (-\beta_1\nabla D(\mathbf{q}_1), -\beta_2\nabla D(\mathbf{q}_2), \dots, -\beta_N\nabla D(\mathbf{q}_N))$$

on the cone of feasible velocities:

$$\frac{d\mathbf{q}}{dt} = P_{C_\mathbf{q}}\left(-\nabla\Phi_\beta(\mathbf{q})\right), \tag{18}$$

which can be written

$$\frac{d\mathbf{q}}{dt} \in -\partial\left(\Phi_\beta(\mathbf{q}) + I_K(\mathbf{q})\right).$$

Strictly speaking, the gradient flow nature of the evolution process is lost, since $\beta = (\beta_1, \dots, \beta_N) \in [0,1]^N$ may vary in time. We shall not address the full control problem which would consist in looking for an optimal choice of $\beta(t)$ in order to optimize the evacuation. We shall rather investigate possible ways to fluidize the evacuation by prescribing a closed-loop procedure to determine the instantaneous $\beta_i's$, in a way that only depends on local information. More precisely, we seek for a procedure to determine β_i that dynamically depends upon the relative position of individual i with respect to its close neighbors, and upon its frustration, i.e. the deviation between its desired velocity $\mathbf{U}(\mathbf{q}_i)$ and its actual one $\mathbf{u}_i$.

In order to account for the reaction time of individuals, we consider that the coefficient β_i depends on the mean value of the individual frustration (defined by (16)) in the recent past. More precisely, we set

$$\beta_i = 1 - \int_0^t \rho(t-s)\, f_i(t)\, dt, \tag{19}$$

where $\rho(\cdot)$ is a convolution kernel:

$$\rho \ : \ \mathbb{R}^+ \longmapsto \mathbb{R}^+, \ \rho(x) \geq 0 \quad \forall x, \ \int_0^{+\infty} \rho(s)\, ds = 1.$$

We shall simply choose here $\rho = \frac{1}{\eta}\mathbb{1}_{[0,\eta]}$, where η is a typical reaction time. Note that β_i may exit the interval $[0,1]$ in some situations, e.g. when some individuals are pushed forward by people behind them, or when some others are pushed backward. But the typical situation is $f_i \in [0,1]$, which implies $\beta_i \in [0,1]$.

In order to account for the location of individual within the jam, we activate the evolution of β_i only for those who have close neighbors in their angle of vision. More precisely, the modification of β_i is only made active when there is at least another individual $\mathbf{q}_j$ in the angular sector of angle $\theta_v = 60^\circ$ and length $3.5 \times r_i$. Figure 9 illustrates the two situations: The individual at $\mathbf{q}_i$ has two neighbors in his angle of vision, and therefore adapt his β_i according to his frustration, whereas individual i', even if frustated, will continue pushing. Finally, we shall consider that, when a jam is broken and the crowd resumes its motion, all individuals recover their will to walk ahead. Thus, whenever the global frustration F (defined by (17)) drops below a threshold value F_c, the correction previsouly described is desactivated.

The example we propose is based on the evacuation of a square room with a single exit. All individuals point toward the unique exit door. The velocity is defined by (18),

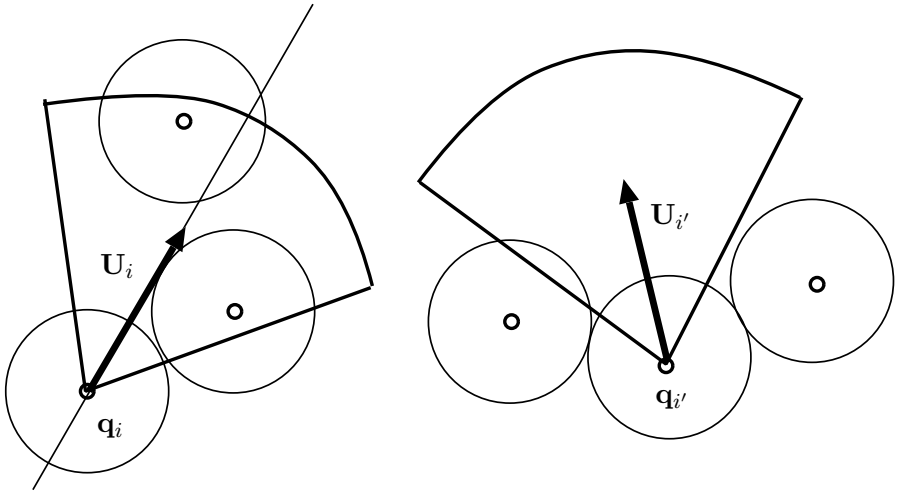

FIGURE 9. Angle of vision, with (right) and without (left) a clear horizon

the correction coefficient $\beta_i's$ by (19), and the individual frustrations $f_i's$ by (16). We integrate the rule that, whenever the mean frustration F (defined by (17)) is less than $F_c = 0.99$, all frustrations are reset to 0. The reaction time η is 1 s. There are initially 363 individuals in the room, and the relative width of the door (with respect to the mean individual diameter) is 1.43. From Fig. 3 in Section 3, it corresponds to a situation where the jamming probability is 1, so that the straight gradient flow evacuation is highly unefficient: the crowd almost instantaneously stops, trapped in a local minimum of the dissatisfaction function.

Fig. 10 plots the evolution of the global dissatisfaction Φ, together with the mean frustration. With this feedback loop strategy, whenever a jam is formed, all frustrations are close to 1, and the corresponding $\beta_i's$ decrease, which destabilizes the jam and resumes the evacuation process, until a new jam is reached. Since a jam corresponds to a local minimum of the satisfaction Φ, this destabilizations occurs at the expense of an *increase* of Φ that can be observed in the figure. This increase is needed to exit the local potential well and dynamically resume the steepest descent process. The highly oscillating curve corresponds to the mean frustration. It oscillates in the very neighborhood of 1 when a jam occurs, then decreases when the jam starts to destabilize. As soon as it drops below the threshold value $F_c = 0.99$, all individuals recover their unrestrained desired velocity, and the jam tumbles. This process occurs 4 times in the evacuation represented by Fig. 10. We stress the paradoxical character of the effect that is created by the feedbak loop strategy: A *reduction* of the desired velocities fluidizes the evacuation, i.e., *increases* the mean velocity of the crowd (converse of the *Faster is Slower* effect [19, 36]).

6. Computations in realistic situation

In order to illustrate the praticality of this approach to handle real life situation, we end this paper by an evacuation scenario in a more complex situation, namely an exhibition area in Paris. The dissatisfaction function $D(\cdot)$, that is the geodesic distance to the exit, is computed by a Fast Marching Method [42]. Isolines of the computed field D are plotted in Fig. 11 (top). The bottom figure represents a snapshot of the crowd during evacuation. The arrows represent the desired velocities ($\mathbf{U}_i = -\nabla D(\mathbf{q}_i)$ for an individual at $\mathbf{q}_i$).

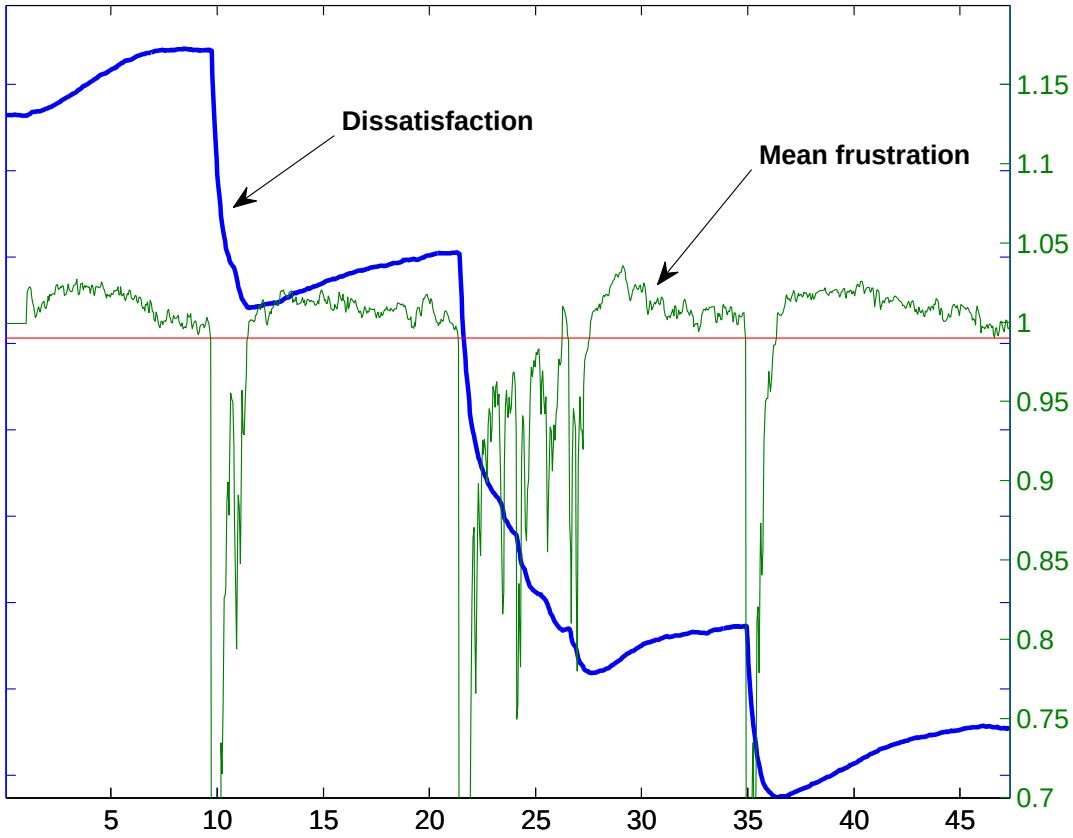

FIGURE 10. Global dissatisfaction Φ (and mean frustration F) *vs.* time

7. CONCLUSION

We have attempted here to show how a purely granular and greedy crowd motion model without any friction effects can explain complicated effects that are observed in experimental or real life crowd flows. The core of the model relies on a simple gradient flow principle, based on the constrained dissatisfaction function

$$\Psi = \Phi + I_K,$$

where Φ expresses the sum of individual dissatisfactions, and I_K forbids overlapping. Whereas Φ is convex in general (e.g. for individuals heading to a single exit), the feasible set K is not, so that the global function Ψ is never convex. In this setting, it may happen that the gradient flow $t \mapsto \mathbf{q}(t)$ is stuck in a local minimum, which leads to a static solution, and thereby an infinite evacuation time. We showed that this phenomenon corresponds to very special, namely hyperstatic, configurations. They systematically occur when the door is smaller than twice the people diameter, almost never when the relative width of the door is larger than 2.7, and occasionally when the door width lies in between. Increasing desired velocity (frustrated people tend to push further) is likely to overstabilize these jams, whereas a *decrease* of some desired velocity can help the overall crowd to exit the attraction bassin of the local minimum, thereby resuming the evacuation process (*Slower is Faster* effect), as shown in section 5.

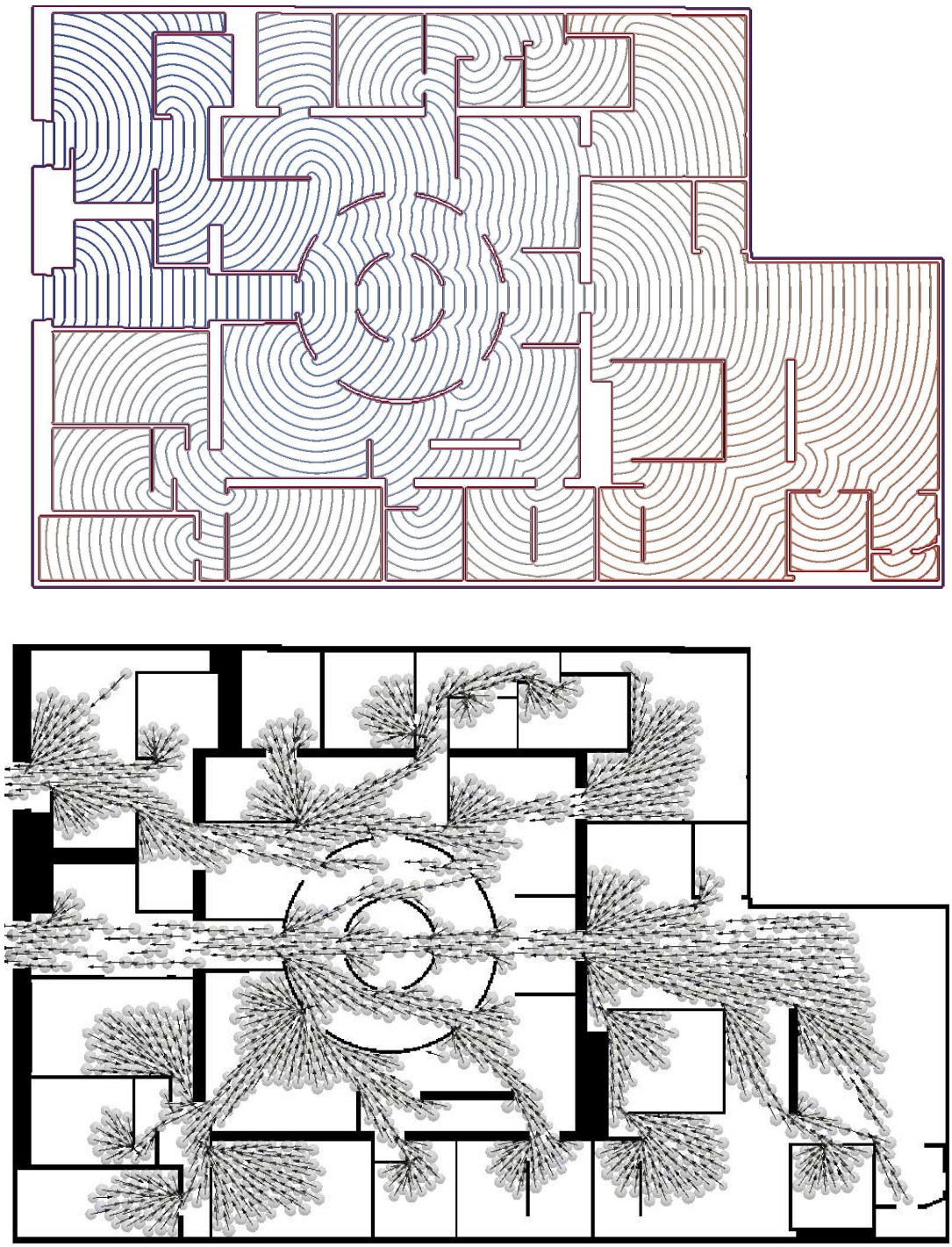

FIGURE 11. Evacuation of an exhibition area: Isovalues of Φ (top), and velocity field (bottom)

In situations where static jams do not occur, the crowd (represented by the vector $\mathbf{q}$) sometimes passes in the neighborhood of unstable jam configurations, that corresponds to saddle-points for the functional Ψ. When this happens, the evacuation process is significantly slowed down, until $\mathbf{q}$ escapes from this saddle-point neighborhood by slipping along unstable directions (corresponding to negative eigenvalues of the Hessian matrix). This allows to reproduce *Stop-and-Go* waves with a minimal set of assumptions, and in particular without assuming any change in individual strategies.

Appendix A. Computation of the Hessian matrix

We detail here the computation of the Hessian matrix H_ε of Ψ_ε.

$$\Psi_\varepsilon \,:\, \mathbf{q} \in \mathbb{R}^{2N} \longmapsto \Psi_\varepsilon(\mathbf{q}) = \sum_{i=1}^{N} |\mathbf{q}_i - \mathbf{q}_{\infty i}| + \frac{1}{2\varepsilon} \sum_{i \neq j} (|\mathbf{q}_j - \mathbf{q}_i| - r_i - r_j)_-^2.$$

The gradient of Ψ_ε is

$$\nabla \Psi_\varepsilon = \sum_{i=1}^{N} \mathbf{e}_{\infty i}^i - \frac{1}{\varepsilon} \sum_{i \sim j} (r_i + r_j - |\mathbf{q}_j - \mathbf{q}_i|)(\mathbf{e}_{ij}^j - \mathbf{e}_{ij}^i).$$

The basic ingredient of the computation is the following: considering two individuals at $\mathbf{q}_i$ and $\mathbf{q}_j$, and the associated unit vector

$$\mathbf{e}_{ij} = \frac{\mathbf{q}_j - \mathbf{q}_i}{|\mathbf{q}_j - \mathbf{q}_i|} = \nabla_{\mathbf{q}_j} |\mathbf{q}_j - \mathbf{q}_i| = -\nabla_{\mathbf{q}_i} |\mathbf{q}_j - \mathbf{q}_i| \,,$$

the gradient of $\mathbf{e}_{ij}$ with respect to $\mathbf{q}_j$ is the 2×2 rank-1 matrix

$$\nabla_{\mathbf{q}_i} \mathbf{e}_{ij} = \mathbf{e}_{ij}^\perp \otimes \mathbf{e}_{ij}^\perp,$$

and the gradient with respect to $\mathbf{q}_i$ is the opposite.

The contribution of the dissatisfaction term to the Hessian is

$$\nabla \left(\sum_{i=1}^{N} \mathbf{e}_{\infty i}^i \right) = \sum_{i=1}^{N} \frac{1}{|\mathbf{q}_i - \mathbf{q}_i^\infty|} \mathbf{e}_{\infty i}^\perp.$$

Let us now evaluate the contribution of the penalty term that accounts for the non-overlapping constraints. For any i and j such that $i \sim j$, it holds that

$$\begin{aligned} \nabla_{\mathbf{q}_i} \left(\frac{1}{\varepsilon} (|\mathbf{q}_j - \mathbf{q}_i| - r_i - r_j)\, \mathbf{e}_{ij}^i \right) &= +\frac{1}{\varepsilon} \mathbf{e}_{ij}^i \otimes \mathbf{e}_{ij}^i \\ &- \underbrace{\frac{1}{\varepsilon} (r_i + r_j - |\mathbf{q}_j - \mathbf{q}_i|)}_{\approx \lambda_{ij}} \frac{1}{|\mathbf{q}_i - \mathbf{q}_j|} \mathbf{e}_{ij}^{\perp i} \otimes \mathbf{e}_{ij}^{\perp i}. \end{aligned}$$

Similarly,

$$\nabla_{\mathbf{q}_i} \left(-\frac{1}{\varepsilon} (|\mathbf{q}_j - \mathbf{q}_i| - r_i - r_j)\, \mathbf{e}_{ij}^j \right) = -\frac{1}{\varepsilon} \mathbf{e}_{ij}^j \otimes \mathbf{e}_{ij}^i + \frac{\lambda_{ij}}{|\mathbf{q}_i - \mathbf{q}_j|} \mathbf{e}_{ij}^{\perp j} \otimes \mathbf{e}_{ij}^{\perp i}.$$

Summing up all contributions, we obtain the full expression (15).

Acknowledgment

The authors would like to thank A. Lefebvre, A. Roudneff-Chupin, F. Santambrogio, L. Thibault, and J. Venel for interesting discussions and suggestions. Both authors are partially supported by ANR project Isotace (ANR-12-MONU-0013).

References

[1] P. Ballard, The dynamics of discrete mechanical systems with perfect unilateral constraints, *Arch. Ration. Mech. Anal.* **154(3)** (2000) 199–274.

[2] N. Bellomo and C. Dogbé, On the modelling crowd dynamics from scaling to hyperbolic macroscopic models, *Math. Models Methods Appl. Sci.* **18** (2008) 1317–1345.

[3] N. Bellomo, A. Bellouquid and D. Knopoff, From the microscale to collective crowd dynamics, *Multiscale Model. Simul.* **11(3)** (2013) 943–963.

[4] F. Bouchut, Y. Brenier, J. Cortes and J.-F. Ripoll, A hierarchy of models for two-phase flows, *J. Nonlinear Sci.* **10(6)** (2000) 639–660.

[5] M. Bounkhel and L. Thibault, Nonconvex sweeping process and prox-regularity in Hilbert space, *J. Nonlinear Convex Anal.* **6(2)** (2005) 359–374.

[6] Y. Brenier and E. Grenier, Sticky particles and scalar conservation laws, *SIAM J. Numer. Anal.* **35(6)** (1998) 2317–2328.

[7] M. Burger, P. A. Markowich, and J.-F. Pietschmann, Continuous limit of a crowd motion and herding model: Analysis and numerical simulations, *Kinet. Relat. Models* **4(4)** (2011) 1025–1047.

[8] C. Burstedde, K. Klauck, A. Schadschneider and J. Zittartz, Simulation of pedestrian dynamics using a two-dimensional cellular automaton, *Physica A: Statistical Mechanics and its Applications* **295(3-4)** (2001) 507–525.

[9] C. Chalons, P. Goatin and N. Seguin, General constrained conservation laws. Application to pedestrian flow modeling. *Netw. Heterog. Media* **8(2)** (2013) 433–463.

[10] R. Colombo, M. Garavello and M. Lécureux-Mercier, A class of nonlocal models for pedestrian traffic, *Math. Models Methods Appl. Sci.* **22(4)** (2012) 1150023.

[11] E. Cristiani, B. Piccoli and A. Tosin, Multiscale modeling of granular flows with application to crowd dynamics, *Multiscale Model. Simul.* **9(1)** (2011) 155–182.

[12] P. Degond, C. Appert-Rolland, J. Pettré and G. Theraulaz, Vision-based macroscopic pedestrian models, *Kinet. Relat. Models* **6(4)** (2013) 809–839.

[13] D.C. Duives, W. Daamen and S. P. Hoogendoorn, State-of-the-art crowd motion simulation models, *Transportation Research Part C: Emerging Technologies* **37** (2013) 193–209.

[14] H. Federer, Curvature measures, *Trans. Amer. Math. Soc.* **93** (1959) 418–491.

[15] P.G. Gipps and B. Marksjö, A micro-simulation model for pedestrian flows, *Mathematics and Computers in Simulation* **27(2-3)** (1985) 95–105.

[16] E.T. Hall, *The hidden dimension*, (Garden City, N.Y. : Doubleday, 1966).

[17] D. Helbing, A fluid-dynamic model for the movement of pedestrians, *Complex Systems* **6(5)** (1992) 391–415.

[18] D. Helbing, I. Farkas and T. Vicsek, Simulating dynamical features of escape panic, *Nature* **407** (2000) 487–490.

[19] D. Helbing and A. Johansson, Pedestrian, crowd and evacuation dynamics, *Extreme Environmental Events* (2011) 697–716.

[20] D. Helbing and P. Molnár, Social force model for pedestrian dynamics, *Phys. Rev E* **51(5)** (1995) 4282–4286.

[21] S.P. Hoogendoorn and P.H.L. Bovy, Continuum modeling of multiclass traffic flow, *Transportation Research Part B: Methodological* **34(2)** (2000) 123–146.

[22] S.P. Hoogendoorn and P.H.L. Bovy, Generic gas-kinetic traffic systems modeling with applications to vehicular traffic flow, *Transportation Research Part B: Methodological* **35(4)** (2001) 317–336.

[23] R.L. Hughes, A continuum theory for the flow of pedestrians, *Transportation Research Part B: Methodological* **36(6)** (2002) 507–535.

[24] A.U. Kemloh Wagoum, A. Seyfried and S. Holl, Modeling the dynamic route choice of pedestrians to assess the criticality of building evacuation, *Adv. Complex Syst.* **15(7)** (2012) 1250029.

[25] B. Maury, Non smooth evolution models in crowd dynamics: Mathematical and numerical issues, in *Collective Dynamics from Bacteria to Crowds, An Excursion Through Modeling, Analysis and Simulation*, Series: CISM International Centre for Mechanical Sciences, Vol. 553 (2014)

[26] B. Maury, A time-stepping scheme for inelastic collisions, *Numer. Math.* **102(4)** (2006) 649–679.

[27] B. Maury, Prise en compte de la congestion dans les modèles de mouvements de foules, *Actes des Colloques Caen 2012-Rouen 2011.*

[28] B. Maury, A. Roudneff-Chupin and F. Santambrogio, A macroscopic crowd motion model of gradient flow type, *Math. Models Methods Appl. Sci.* **20(10)** (2010) 1787–1821.

[29] B. Maury, A. Roudneff-Chupin, F. Santambrogio and J. Venel, Handling congestion in crowd motion modeling, *Netw. Heterog. Media* **6(3)** (2011) 485–519.
[30] B. Maury and J. Venel, A mathematical framework for a crowd motion model, *C. R. Math. Acad. Sci. Paris* **346(23-24)** (2008) 1245–1250.
[31] B. Maury and J. Venel, A discrete contact model for crowd motion, *ESAIM Math. Model. Numer. Anal.* **45(1)** (2011) 145–168.
[32] M. Mazade and L. Thibault, Regularization of differential variational inequalities with locally prox-regular sets, *Math. Program., Ser. B* **139(1-2)** (2013) 243–269.
[33] J.-J. Moreau, Décomposition orthogonale d'un espace hilbertien selon deux cônes mutuellement polaires, *C. R. Acad. Sci. Paris* **255** (1962) 238–240.
[34] J.-J. Moreau, Evolution problem associated with a moving convex set in a Hilbert space, *J. Differential Equations* **26(3)** (1977) 347–374.
[35] J.-J. Moreau, Some numerical methods in multibody dynamics: application to granular materials, *European J. Mech. A Solids* **13(4)** (1994) 93–114.
[36] D.R. Parisi and C.O. Dorso, Why "Faster is Slower" in Evacuation Process, *Pedestrian and Evacuation Dynamics 2005, Springer* (2007) 341–346.
[37] D.R. Parisi, M. Gilman and H. Moldovan, A modification of the Social Force Model can reproduce experimental data of pedestrian flows in normal conditions, *Physica A: Statistical Mechanics and its Applications* **388(17)** (2009) 3600–3608.
[38] P. Pécol, S. Dal Pont, S. Erlicher and P. Argoul, Smooth/non-smooth contact modeling of human crowds movement: Numerical aspects and application to emergency evacuations, *Ann. Solid Struct. Mech.* **2** (2011) 69–85.
[39] B. Piccoli and A. Tosin, Time-evolving measures and macroscopic modeling of pedestrian flow, *Arch. Rational Mech. Anal.* **199** (2011) 707–738.
[40] R.A. Poliquin, R.T. Rockafellar and L. Thibault, Local differentiability of distance functions, *Trans. Amer. Math. Soc.* **352(11)** (2000) 5231–5249.
[41] A. Schadschneider and A. Seyfried, Empirical results for pedestrian dynamics and their implications for cellular automata models, *Pedestrian behavior: models, data collection and applications, Ed.: H. Timmermans, Emerald* (2009) 27–44.
[42] J.A. Sethian, *Level Set Methods and Fast Marching Methods*, (Cambridge University Press, Cambridge, UK, 1999).
[43] L. Thibault, Sweeping process with regular and nonregular sets, *J. Differential Equations* **193(1)** (2003) 1–26.
[44] J. Venel, Integrating strategies in numerical modelling of crowd motion, *Pedestrian and Evacuation Dynamics 2008, Springer* (2010) 641–646.
[45] J. Venel, A numerical scheme for a class of sweeping processes, *Numer. Math.* **118(2)** (2011) 367–400.
[46] H. Xi, Y.-L. Son and S. Lee, An integrated pedestrian behavior model based on extended decision field theory and social force model. *Simulation Conference (WSC), Proceedings of the 2010 Winter, B. Johansson, S. Jain, J. Montoya-Torres, J. Hugan, and E. Ycesan, eds.* (2010) 824–836.